

# Lysine methylation shields an intracellular pathogen from ubiquitylation

Patrik Engström<sup>1\*</sup>, Thomas P. Burke<sup>1</sup>, Anthony T. Iavarone<sup>2</sup>, Matthew D. Welch<sup>1\*</sup>

<sup>1</sup>Department of Molecular and Cell Biology, University of California, Berkeley, CA 94720, USA.

<sup>2</sup>QB3/Chemistry Mass Spectrometry Facility, University of California, Berkeley, CA 94720, USA.

\*Correspondence to: [pengstrom@berkeley.edu](mailto:pengstrom@berkeley.edu) (P.E.), [welch@berkeley.edu](mailto:welch@berkeley.edu) (M.D.W).

## 1 Abstract

2 Many intracellular pathogens avoid detection by their host cells. However, it remains  
3 unknown how they avoid being tagged by ubiquitin, an initial step leading to anti-microbial  
4 autophagy. Here, we show that the intracellular bacterial pathogen *Rickettsia parkeri* uses  
5 two protein-lysine methyltransferases (PKMTs) to modify outer membrane proteins (OMPs) and  
6 prevent their ubiquitylation. Mutants deficient in the PKMTs were avirulent in mice and failed to  
7 grow in macrophages due to ubiquitylation and autophagy. Analysis of the lysine-methylome  
8 revealed that PKMTs modify a subset of OMPs by methylation at the same sites that are recognized  
9 by host ubiquitin. These findings show that lysine methylation is an essential determinant of  
10 rickettsial pathogenesis that shields bacterial proteins from ubiquitylation to evade autophagic  
11 targeting.

## 12 Main

13           Intracellular pathogens generally evade the host immune surveillance machinery. This  
14    includes avoidance of surface targeting by the host ubiquitylation machinery and subsequent  
15    formation of a polyubiquitin coat, a first step in cell-autonomous immunity (1-5). The ubiquitin  
16    coat recruits autophagy receptors that engage with the autophagy machinery to target cytosol-  
17    exposed microbes for destruction (1, 4-8). Bacterial outer membrane proteins (OMPs) are targets  
18    for the host ubiquitylation machinery (9, 10), and the tick-borne obligate intracellular pathogen  
19    *Rickettsia parkeri* requires the abundant surface protein OmpB to protect OMPs from  
20    ubiquitylation (11). However, the detailed mechanisms that *R. parkeri* and other pathogens use to  
21    block lysine ubiquitylation of surface proteins, including OMPs, are unknown. We hypothesized  
22    that cell surface structures or modifications could provide protection at the molecular level. One  
23    such modification is lysine methylation, which is widespread in all domains of life. This  
24    modification involves the transfer of one, two, or three methyl groups to the amino group of lysine  
25    side chains, the same amino group that can also be modified by ubiquitin (12). Whether lysine  
26    methylation of bacterial surfaces prevents host detection and promotes intracellular survival has  
27    not been explored.

28           To identify bacteria-derived surface modifications that protect against ubiquitin coating,  
29    we screened a library of *R. parkeri* transposon mutants (13) (**Table S1**) for increased  
30    polyubiquitylation (pUb) relative to wild-type (WT) in Vero cells (an epithelial cell line commonly  
31    used to propagate and study intracellular pathogens) by immunofluorescence microscopy (**Fig.**  
32    **1A**). We subsequently analyzed individual mutants and identified 4 that were ubiquitylated, similar  
33    to *ompB* mutant bacteria (11) (**Fig. 1B and D**). Importantly, these 4 strains expressed OmpB (**Fig.**  
34    **S1**). Two of the strains had insertions in the protein-lysine methyltransferase genes *pkmt1* and

35 *pkmt2*, which are located in two distinct chromosomal regions. The remaining two strains had  
36 insertions in the *wecA* and *rmlD* genes, which are required for the biosynthesis of O-antigen (**Fig.**  
37 **S2**), a common surface molecule in Gram-negative bacteria. The O-antigen also protects  
38 *Francisella tularensis* from ubiquitylation (5), suggesting it performs a conserved function in this  
39 process. As a control, we analyzed a strain with a mutation in the *mrdA* gene, which is required  
40 for peptidoglycan biosynthesis and cell shape in other bacteria (14). This mutant strain had altered  
41 shape but was not polyubiquitylated (**Fig. 1B and D**), suggesting that not all bacterial cell envelope  
42 structures are required to avoid ubiquitylation. In addition, we further quantified the pUb levels  
43 and observed that the *pkmt1::tn* mutant, followed by the *ompB* and *pkmt2::tn* mutants, had the  
44 highest levels (**Fig. 1E**). These data indicated that OmpB, PKMTs, and the O-antigen protect *R.*  
45 *parkeri* from ubiquitylation.

46 The O-antigen was previously shown to be required for rickettsial pathogenesis (15), and  
47 OmpB was previously found to be required for *R. parkeri* to cause lethal disease in *Ifnar<sup>-/-</sup>Ifngr<sup>-/-</sup>*  
48 mice lacking the type I interferon receptor (IFNAR) and IFN-g receptor (IFNGR) (16). We  
49 therefore examined whether PKMT1 or PKMT2 are important for causing disease *in vivo*. We  
50 observed that *Ifnar<sup>-/-</sup>Ifngr<sup>-/-</sup>* mice succumbed to infection with WT but not to *pkmt1::tn* or *pkmt2::tn*  
51 bacteria (**Fig. 1F**). Mice infected with the *pkmt1::tn* mutant showed no signs of disease, whereas  
52 mice infected with *pkmt2::tn* showed a transient loss in body weight (**Fig. S3**). This indicates that  
53 PKMT1 and PKMT2 are determinants of *R. parkeri* pathogenesis.

54 Because PKMT1 or PKMT2 had previously been shown to methylate OmpB *in vitro* (17-  
55 20), we next examined whether methylation protects OmpB, or another abundant outer membrane  
56 protein OmpA (21), from ubiquitylation. First, Vero cells overexpressing 6xHis-tagged ubiquitin  
57 were infected with WT and the *ompB*, *pkmt1::tn*, and *pkmt2::tn* strains. 6xHis-tagged ubiquitin

58 was recruited to the surface of all of the mutants, but not WT bacteria, as observed by  
59 immunofluorescence microscopy (**Fig. 2A**). Then, 6xHis-ubiquitylated proteins were affinity-  
60 purified from infected cells, and OmpA and OmpB were detected by western blotting. OmpA was  
61 shifted towards higher molecular weights in cells infected with mutant, but not WT bacteria,  
62 indicating OmpA is ubiquitylated (**Fig. 2B**). Similarly, in comparison with WT bacteria, OmpB  
63 was also shifted towards higher as well as lower molecular weights in cells infected with the  
64 *pkmt1::tn* and *pkmt2::tn* mutants, suggesting that OmpB is ubiquitylated (**Fig. 2B**). To confirm that  
65 methylation protects OmpB and OmpA from ubiquitylation on the bacterial surface, we performed  
66 pUb-enrichments of surface fractions from purified bacteria followed by western blotting. This  
67 revealed that both OmpB and OmpA shifted towards higher molecular weights in the  
68 methyltransferase mutants but not in WT bacteria (**Fig. 2C**). Thus, methylation is critical to protect  
69 OMPs from ubiquitylation on the bacterial surface.

70 Based on our observation that methylation protects both OmpA and OmpB from  
71 ubiquitylation, we set out to determine how frequently, and to what extent, lysines of *R. parkeri*  
72 OMPs are methylated. Peptides with methylated lysines from whole WT bacteria were quantified  
73 using label-free liquid chromatography-mass spectrometry (LC-MS). We then analyzed lysine  
74 methylation frequency in abundant OMPs as well as other abundant *R. parkeri* proteins (**Table**  
75 **S2**). This analysis revealed that *R. parkeri* OmpB, OmpA, and surface cell antigen 2 (Sca2)  
76 proteins had the highest abundance of methylated peptides. Lysine methylation was also detected  
77 in the outer-membrane assembly protein BamA and in a predicted outer membrane protein porin  
78 (WP\_014410329.1; from here on referred to as OMP-porin) (**Fig. 3A** and **Table S3**). We next  
79 mapped both methylated and unmethylated lysines on the above-mentioned OMPs and found that  
80 more than 50% of lysines detected from OmpB and OmpA were methylated, and a significant

81 fraction of lysines were also methylated in Sca2 (31%), OMP-porin (30%), and BamA (27%) (**Fig.**  
82 **3B** and **Fig. S4**). Thus, in *R. parkeri*, lysine methylation of OMPs is common.

83 To identify OMPs that are methylated by PKMT1 and PKMT2 during infection, we  
84 compared lysine methylation frequencies in WT with those of *pkmt1::tn* or *pkmt2::tn* mutant  
85 bacteria using LC-MS. We found that monomethylation of OmpB, OmpA, the predicted OMP-  
86 porin, and another surface cell antigen protein Sca1 were reduced in *pkmt1::tn* compared to WT  
87 bacteria (**Fig. 3C** and **Fig. S5**). Dimethylation of rickettsial surface proteins was not reduced in the  
88 mutants (**Fig. S6**). Although trimethylation was rare and therefore difficult to analyze at the  
89 individual protein level (**Fig. S6**), OmpB had reduced trimethylation levels in both  
90 methyltransferase mutants (**Fig. 3C**). Notably, the frequency of unmethylated lysines in OmpB  
91 was specifically increased in *pkmt1::tn* bacteria (**Fig. 3C** and **Fig. S5**). Lysine methylation of five  
92 other surface proteins (Sca1, Sca2, BamA, LomR, and Pal-lipoprotein), and 21 of 23 abundant  
93 proteins with different predicted subcellular distributions, was not affected by mutations in the  
94 *pkmt1* or *pkmt2* genes (**Fig. S5**). These data indicate that the PKMTs are required for methylation  
95 of a specific subset of OMPs including OmpB.

96 To determine which OmpB residues are modified by PKMT1 and PKMT2 during *R.*  
97 *parkeri* infection, we analyzed the methylation frequency of individual lysines in the mutants  
98 compared to WT using LC-MS. We observed reduced monomethylation frequencies of OmpB  
99 K418, K623, K634, K902, K1061, K1294, and K1323 in *pkmt1::tn* bacteria compared with WT,  
100 and reduced trimethylation frequencies on K1061 and K388 in the *pkmt2::tn* strain (**Fig. 3D**).  
101 These data indicate that several lysines in *R. parkeri* OmpB are methylated by PKMT1 and  
102 PKMT2 during infection. Although these results were consistent with previous biochemical results  
103 indicating that PKMT1 monomethylates and PKMT2 trimethylates OmpB's lysines (17, 19), we

104 found that total OmpB-methylation is unaffected in the *pkmt2::tn* mutant. This suggests that  
105 PKMT1 is a primary methyltransferase for OmpB and that it can compensate, at least partly, for a  
106 deficiency in PKMT2.

107 To test the hypothesis that methylation of specific lysines in OmpB shields the same  
108 residues from ubiquitylation, we performed pUb-enrichments of bacterial surface fractions  
109 followed by LC-MS to quantify lysines with diglycine (diGly) remnants, a signature for ubiquitin  
110 after trypsin digestion. A prediction of this hypothesis is that individual lysines that are heavily  
111 methylated in OmpB of *Rickettsia* species (17), including WT *R. parkeri* (**Fig. 3D**), are targets for  
112 ubiquitylation in *pkmt1::tn* bacteria. In support of this hypothesis, OmpB K634 and K623 in  
113 *pkmt1::tn* exhibited 7 to 10,000-fold increased ubiquitylation compared with WT bacteria (**Fig.**  
114 **3E, F and Fig. S7; Table S4**). Furthermore, we observed a 13-fold increase in ubiquitylation of  
115 the OMP-porin in *pkmt1::tn* bacteria (**Table S4**), indicating that methylation also protects  
116 additional OMPs. However, in the *pkmt2::tn* mutant, differential OMP-ubiquitylation was below  
117 detection limits (**Fig. 3E, F and Table S4**). Together, these data indicate that methylation by  
118 PKMT1 camouflages lysines in OMPs from ubiquitylation.

119 Because polyubiquitylation promotes recruitment of the autophagy receptors  
120 p62/SQSTM1 and NDP52 (7, 8), we hypothesized that lysine methylation shields OMPs from  
121 ubiquitylation to block recruitment of these proteins. Consistent with this hypothesis, we observed  
122 that the majority of *pkmt1::tn*, *pkmt2::tn*, as well as *ompB* mutant bacteria, co-localized with p62  
123 and NDP52 by immunofluorescence microscopy (**Fig. S8**). These data demonstrate that PKMTs  
124 protect *R. parkeri* from autophagy recognition.

125 Many pathogenic bacteria including *R. parkeri* grow in immune cells such as macrophages  
126 (11), despite the fact that microbial detection in such cells triggers anti-bacterial pathways. We

127 therefore investigated whether PKMT1 or PKMT2 were required for evading autophagy targeting  
128 and bacterial growth in cultured bone marrow-derived macrophages (BMDMs), as was observed  
129 for OmpB (11). BMDMs were generated from control mice and mice lacking the gene encoding  
130 for autophagy related 5 (ATG5), a protein required for optimal membrane envelopment around  
131 pathogens targeted by autophagy, and for their subsequent destruction (6). We observed that  
132 *pkmt1*::tn mutant bacteria were unable to grow in control BMDMs (*Atg5*<sup>fl/fl</sup>), and that growth  
133 was rescued in *Atg5*-deficient BMDMs (*Atg5*<sup>-/-</sup>). Further, >91% of *pkmt1*::tn bacteria were labeled  
134 with both pUb and p62 in *Atg5*-deficient BMDMs (**Fig. 4A, B, C and D**), suggesting that ubiquitin-  
135 tagged bacteria were not restricted when the autophagy cascade was prevented. In contrast, the  
136 *pkmt2*::tn mutant did not have a major growth defect compared with WT bacteria and 50% of the  
137 bacteria were labeled with p62, irrespective of host genotype (**Fig. 4A, B, C and D**), consistent  
138 with less pronounced ubiquitylation phenotypes compared to *pkmt1*::tn bacteria. Collectively,  
139 these data indicate that methylation is required for *R. parkeri* growth in macrophages by avoiding  
140 autophagic targeting.

141 Our work reveals a detailed molecular mechanism that camouflages bacterial surface  
142 proteins from host detection. In particular, we found that lysine methylation was essential for  
143 blocking ubiquitylation, a first step in cell-autonomous immunity (1-4). This highlights an intricate  
144 evolutionary arms race between pathogens and hosts and reveals a strategy that pathogens can  
145 adapt to counteract host responses. The lysine methyltransferases PKMT1 and PKMT2 are  
146 conserved between rickettsial species (**Fig. S9** and **Fig. S10**) and contain a core Rossmann fold  
147 found in the broader superfamily of class I methyltransferases that exist in diverse organisms (12,  
148 18). Thus, we propose that lysine methylation, and potentially other lysine modifications, could be  
149 used by pathogens, symbionts, and perhaps even in eukaryotic organelles, to prevent undesirable

150 surface ubiquitylation and downstream consequences including elimination by autophagy. Further  
151 study of microbial surface modifications will continue to enhance our understanding of the  
152 pathogen-host interface and could ultimately lead to new therapeutic targets for treating human  
153 diseases including those caused by infectious agents.

154 **References and Notes**

155 1. F. Rando, R. J. Youle, Self and nonself: how autophagy targets mitochondria and  
156 bacteria. *Cell Host Microbe* **15**, 403-411 (2014).

157 2. A. J. Perrin, X. Jiang, C. L. Birmingham, N. S. So, J. H. Brumell, Recognition of bacteria  
158 in the cytosol of Mammalian cells by the ubiquitin system. *Curr Biol* **14**, 806-811 (2004).

159 3. S. J. L. van Wijk *et al.*, Linear ubiquitination of cytosolic *Salmonella* Typhimurium  
160 activates NF-kappaB and restricts bacterial proliferation. *Nat Microbiol* **2**, 17066 (2017).

161 4. J. Noad *et al.*, LUBAC-synthesized linear ubiquitin chains restrict cytosol-invading  
162 bacteria by activating autophagy and NF-kappaB. *Nat Microbiol* **2**, 17063 (2017).

163 5. E. D. Case *et al.*, The *Francisella* O-antigen mediates survival in the macrophage cytosol  
164 via autophagy avoidance. *Cell Microbiol* **16**, 862-877 (2014).

165 6. J. Huang, J. H. Brumell, Bacteria-autophagy interplay: a battle for survival. *Nat Rev  
166 Microbiol* **12**, 101-114 (2014).

167 7. Y. T. Zheng *et al.*, The adaptor protein p62/SQSTM1 targets invading bacteria to the  
168 autophagy pathway. *J Immunol* **183**, 5909-5916 (2009).

169 8. T. L. Thurston, G. Ryzhakov, S. Bloor, N. von Muhlinen, F. Rando, The TBK1 adaptor  
170 and autophagy receptor NDP52 restricts the proliferation of ubiquitin-coated bacteria. *Nat  
171 Immunol* **10**, 1215-1221 (2009).

172 9. E. Fiskin, T. Bionda, I. Dikic, C. Behrends, Global analysis of host and bacterial  
173 ubiquitinome in response to *Salmonella* Typhimurium infection. *Mol Cell* **62**, 967-981  
174 (2016).

175 10. M. Polajnar, M. S. Dietz, M. Heilemann, C. Behrends, Expanding the host cell  
176 ubiquitylation machinery targeting cytosolic *Salmonella*. *EMBO Rep* **18**, 1572-1585  
177 (2017).

178 11. P. Engström *et al.*, Evasion of autophagy mediated by *Rickettsia* surface protein OmpB is  
179 critical for virulence. *Nat Microbiol* **4**, 2538-2551 (2019).

180 12. S. Lanouette, V. Mongeon, D. Figeys, J. F. Couture, The functional diversity of protein  
181 lysine methylation. *Mol Syst Biol* **10**, 724 (2014).

182 13. R. L. Lamason, N. M. Kafai, M. D. Welch, A streamlined method for transposon  
183 mutagenesis of *Rickettsia parkeri* yields numerous mutations that impact infection. *PLoS  
184 One* **13**, e0197012 (2018).

185 14. B. G. Spratt, A. B. Pardee, Penicillin-binding proteins and cell shape in *E. coli*. *Nature* **254**,  
186 516-517 (1975).

187 15. H. K. Kim, R. Premaratna, D. M. Missiakas, O. Schneewind, *Rickettsia conorii* O antigen  
188 is the target of bactericidal Weil-Felix antibodies. *Proc Natl Acad Sci U S A* **116**, 19659-  
189 19664 (2019).

190 16. T. P. Burke *et al.*, Inflammasome-mediated antagonism of type I interferon enhances  
191 *Rickettsia* pathogenesis. *Nat Microbiol* **5**, 688-696 (2020).

192 17. D. C. H. Yang, A. H. Abeykoon, B. E. Choi, W. M. Ching, P. B. Chock, Outer membrane  
193 protein OmpB methylation may mediate bacterial virulence. *Trends Biochem Sci* **42**, 936-  
194 945 (2017).

195 18. A. H. Abeykoon *et al.*, Structural insights into substrate recognition and catalysis in outer  
196 membrane protein B (OmpB) by protein-lysine methyltransferases from *Rickettsia*. *J Biol  
197 Chem* **291**, 19962-19974 (2016).

198 19. A. Abeykoon *et al.*, Multimethylation of *Rickettsia* OmpB catalyzed by lysine  
199 methyltransferases. *J Biol Chem* **289**, 7691-7701 (2014).

200 20. A. H. Abeykoon *et al.*, Two protein lysine methyltransferases methylate outer membrane  
201 protein B from *Rickettsia*. *J Bacteriol* **194**, 6410-6418 (2012).

202 21. N. F. Noriea, T. R. Clark, T. Hackstadt, Targeted knockout of the *Rickettsia rickettsii*  
203 OmpA surface antigen does not diminish virulence in a mammalian model system. *mBio*  
204 **6**, (2015).

205 22. R. L. Lamason *et al.*, *Rickettsia* Sca4 Reduces Vinculin-Mediated Intercellular Tension to  
206 Promote Spread. *Cell* **167**, 670-683 e610 (2016).

207 23. U. Distler *et al.*, Drift time-specific collision energies enable deep-coverage data-  
208 independent acquisition proteomics. *Nat Methods* **11**, 167-170 (2014).

209 24. R. S. Plumb *et al.*, UPLC/MS(E); a new approach for generating molecular fragment  
210 information for biomarker structure elucidation. *Rapid Commun Mass Spectrom* **20**, 1989-  
211 1994 (2006).

212 25. P. V. Shliaha, N. J. Bond, L. Gatto, K. S. Lilley, Effects of traveling wave ion mobility  
213 separation on data independent acquisition in proteomics studies. *J Proteome Res* **12**, 2323-  
214 2339 (2013).

215 26. S. Nahnsen, C. Bielow, K. Reinert, O. Kohlbacher, Tools for label-free peptide  
216 quantification. *Mol Cell Proteomics* **12**, 549-556 (2013).

217 27. K. A. Neilson *et al.*, Less label, more free: approaches in label-free quantitative mass  
218 spectrometry. *Proteomics* **11**, 535-553 (2011).

219 28. C. I. Carlström *et al.*, (Per)chlorate-reducing bacteria can utilize aerobic and anaerobic  
220 pathways of aromatic degradation with (per)chlorate as an electron acceptor. *mBio* **6**,  
221 (2015).

222 22. R. L. Lamason *et al.*, *Rickettsia* Sca4 Reduces Vinculin-Mediated Intercellular Tension to  
223 Promote Spread. *Cell* **167**, 670-683 e610 (2016).

224 23. U. Distler *et al.*, Drift time-specific collision energies enable deep-coverage data-  
225 independent acquisition proteomics. *Nat Methods* **11**, 167-170 (2014).

226 24. R. S. Plumb *et al.*, UPLC/MS(E); a new approach for generating molecular fragment  
227 information for biomarker structure elucidation. *Rapid Commun Mass Spectrom* **20**, 1989-  
228 1994 (2006).

229 25. P. V. Shliaha, N. J. Bond, L. Gatto, K. S. Lilley, Effects of traveling wave ion mobility  
230 separation on data independent acquisition in proteomics studies. *J Proteome Res* **12**, 2323-  
231 2339 (2013).

232 26. S. Nahnsen, C. Bielow, K. Reinert, O. Kohlbacher, Tools for label-free peptide  
233 quantification. *Mol Cell Proteomics* **12**, 549-556 (2013).

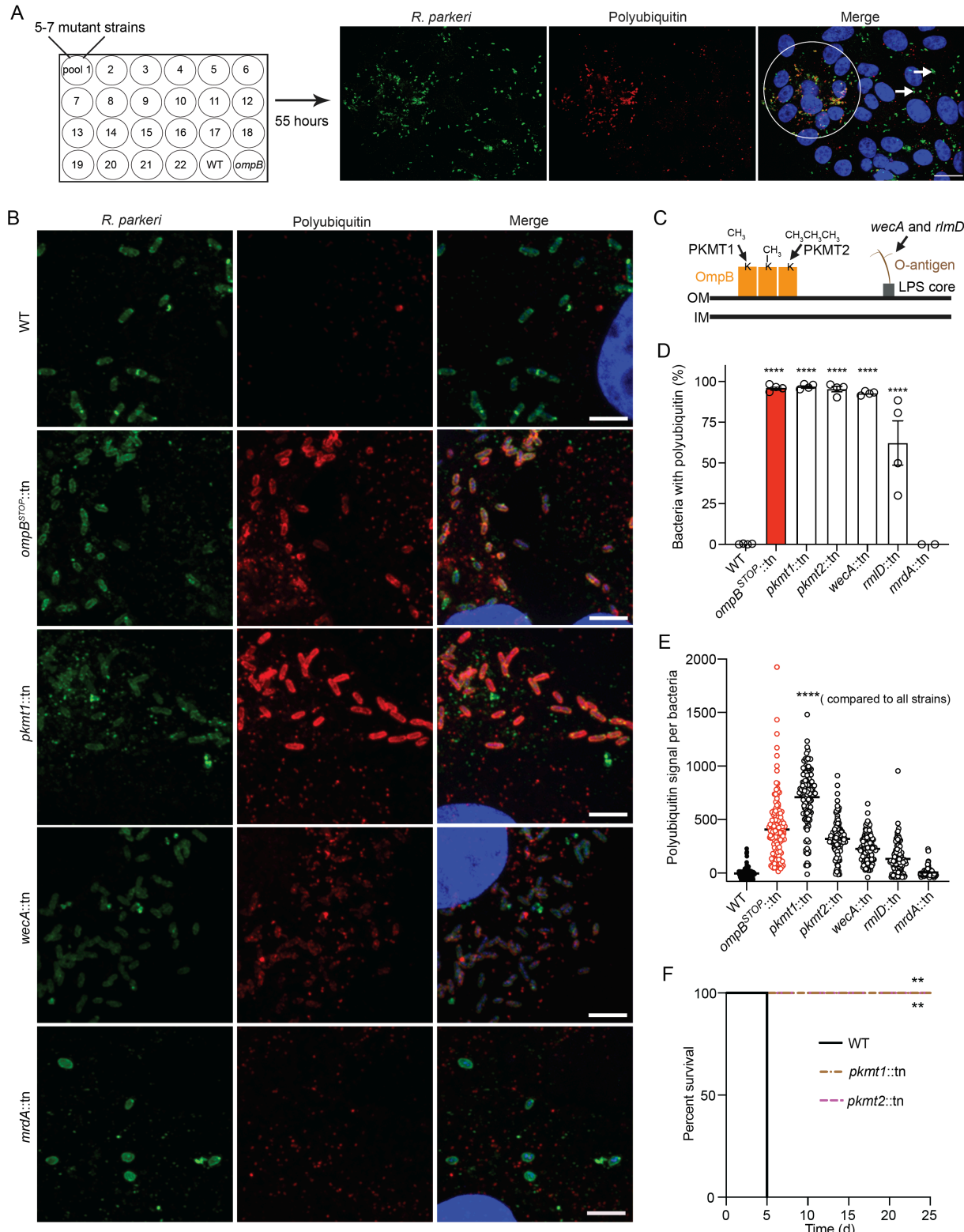
234 27. K. A. Neilson *et al.*, Less label, more free: approaches in label-free quantitative mass  
235 spectrometry. *Proteomics* **11**, 535-553 (2011).

236 28. C. I. Carlström *et al.*, (Per)chlorate-reducing bacteria can utilize aerobic and anaerobic  
237 pathways of aromatic degradation with (per)chlorate as an electron acceptor. *mBio* **6**,  
238 e02287-14 (2015).

239

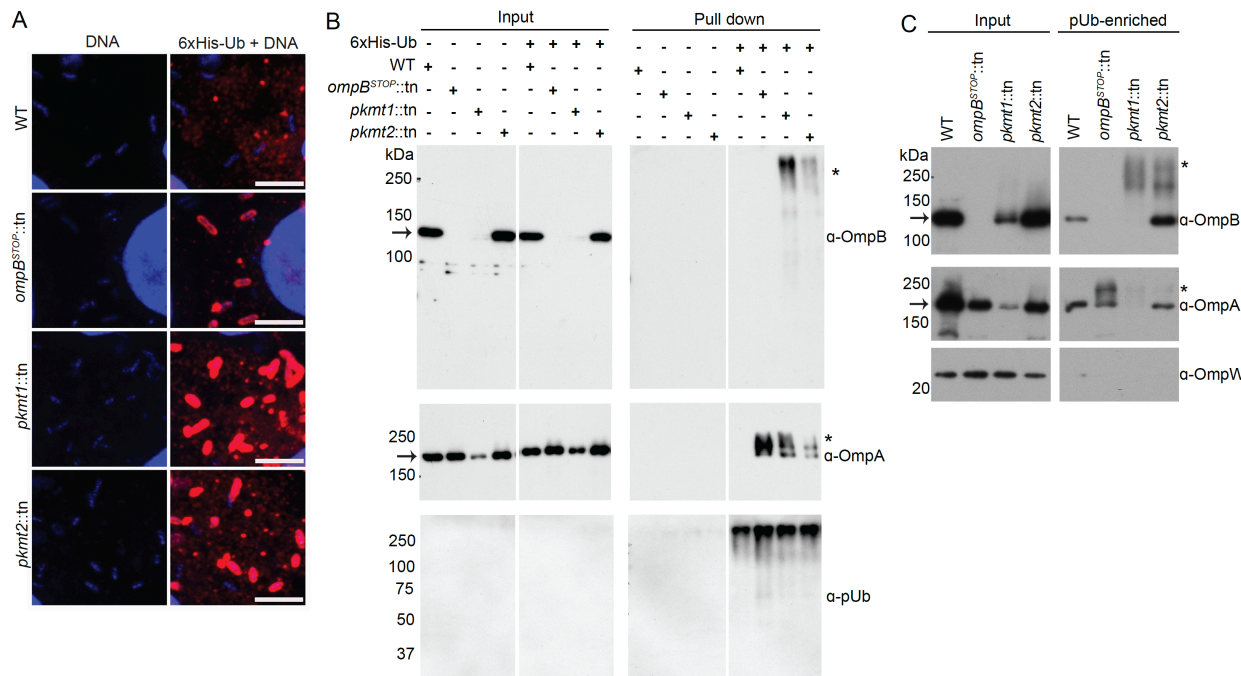
240 **Acknowledgements**

241 We thank Prof. Dan Portnoy (UC Berkeley) and Dr. Lilliana Radoshevich (University of  
242 Iowa) for providing comments on this manuscript, and Neil Fischer (UC Berkeley) for critically  
243 reading the manuscript. We also thank Dr. Hwan Kim (Stony Brook University) for kindly  
244 providing the O-antigen antibody and for fruitful discussions. We are also grateful for the  
245 *Atg5*<sup>fl/fl</sup> and *Atg5*<sup>-/-</sup> BMDMs provided by Dr. G. Golovkine (UC Berkeley), and Profs. Jeffery  
246 S. Cox and Michael Rape (both UC Berkeley) for fruitful discussions. **Funding:** P.E. was  
247 supported by a postdoctoral fellowship from the Sweden-America Foundation. M.D.W. was  
248 supported by NIH/NIAID grants R01 AI109044 and R21 AI138550. A mass spectrometer used in  
249 this study was purchased with support from NIH grant 1S10 OD020062-01. **Author**  
250 **contributions:** P.E. conceived the study with the assistance of M.D.W. P.E. performed laboratory  
251 work and analysis, except for mass spectrometry, which was conducted together with A.T.I., and  
252 animal experiments, which were conducted by T.P.B. P.E. drafted the initial manuscript, and A.T.I.,  
253 T.P.B., and M.W.D provided editorial feedback. **Data and materials availability:** All data used  
254 in the analysis are provided in the main text or supplementary materials. Materials are available  
255 upon request.



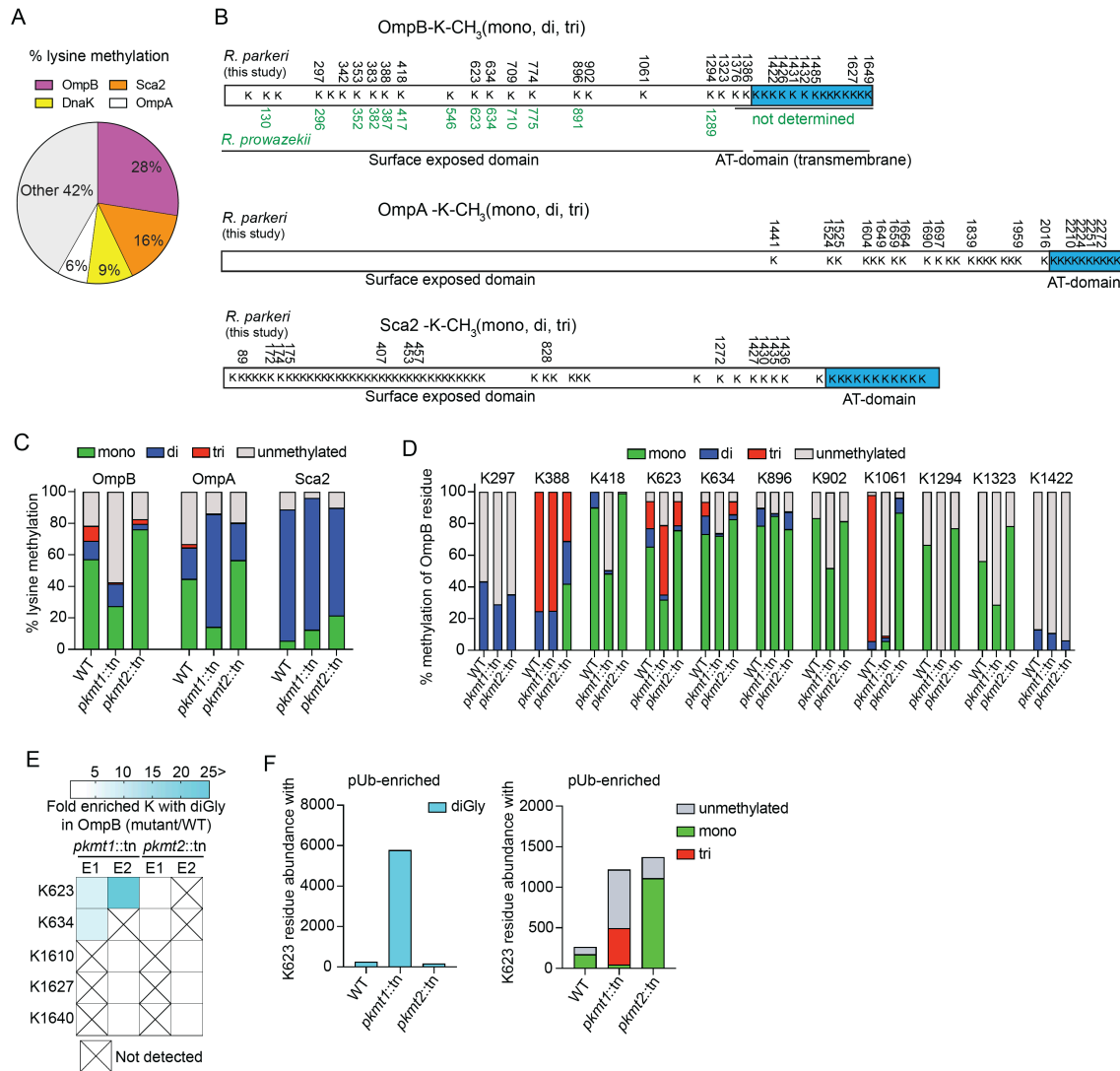
256  
257 **Fig. 1. The O-antigen and lysine methylation are virulence factors that protect *R. parkeri***  
258 **from ubiquitylation.** (A) Pools of *R. parkeri* (green) mutants screened for increased pUb (red)  
259 via immunofluorescence microscopy. DNA, blue. *ompB* mutant (*II*), positive control; WT,

260 negative control. Circle, pUb-positive bacteria; arrows pUb-negative bacteria. Scale bar, 20  $\mu$ m.  
261 (B) Infected cells at 72 hours post-infection (h.p.i.) stained as in A. Scale bar, 5  $\mu$ m ( $n = 4$ ). (C)  
262 Biological function of the genes identified. (D) Percentage of bacteria co-localized with pUb at 72  
263 h.p.i. (Data are the mean  $\pm$  s.e.m.;  $n = 4$  for WT and mutant bacteria; *mrdA*::tn;  $n = 2$ ). Statistical  
264 comparisons between WT and mutants were performed using a one-way ANOVA with Dunnett's  
265 post-hoc test; \*\*\*\*  $P < 0.0001$ . (E) pUb signal per bacteria. (Lines indicate the means;  $n = 3$  fields  
266 of vision). Statistical comparisons were performed using a Kruskal-Wallis test with Dunn's post-  
267 hoc test; \*\*\*\*  $P < 0.0001$ . (F) Survival of *Ifnar*<sup>-/-</sup>/*Ifngr*<sup>-/-</sup> mice intravenously infected with  $5 \times 10^6$   
268 WT or mutant bacteria ( $n = 5$  mice, WT;  $n = 6$  mice, *pkmt1*::tn and *pkmt2*::tn). Statistical  
269 comparison between WT and mutants was performed using a two-way ANOVA; \*\*  $P < 0.01$ .



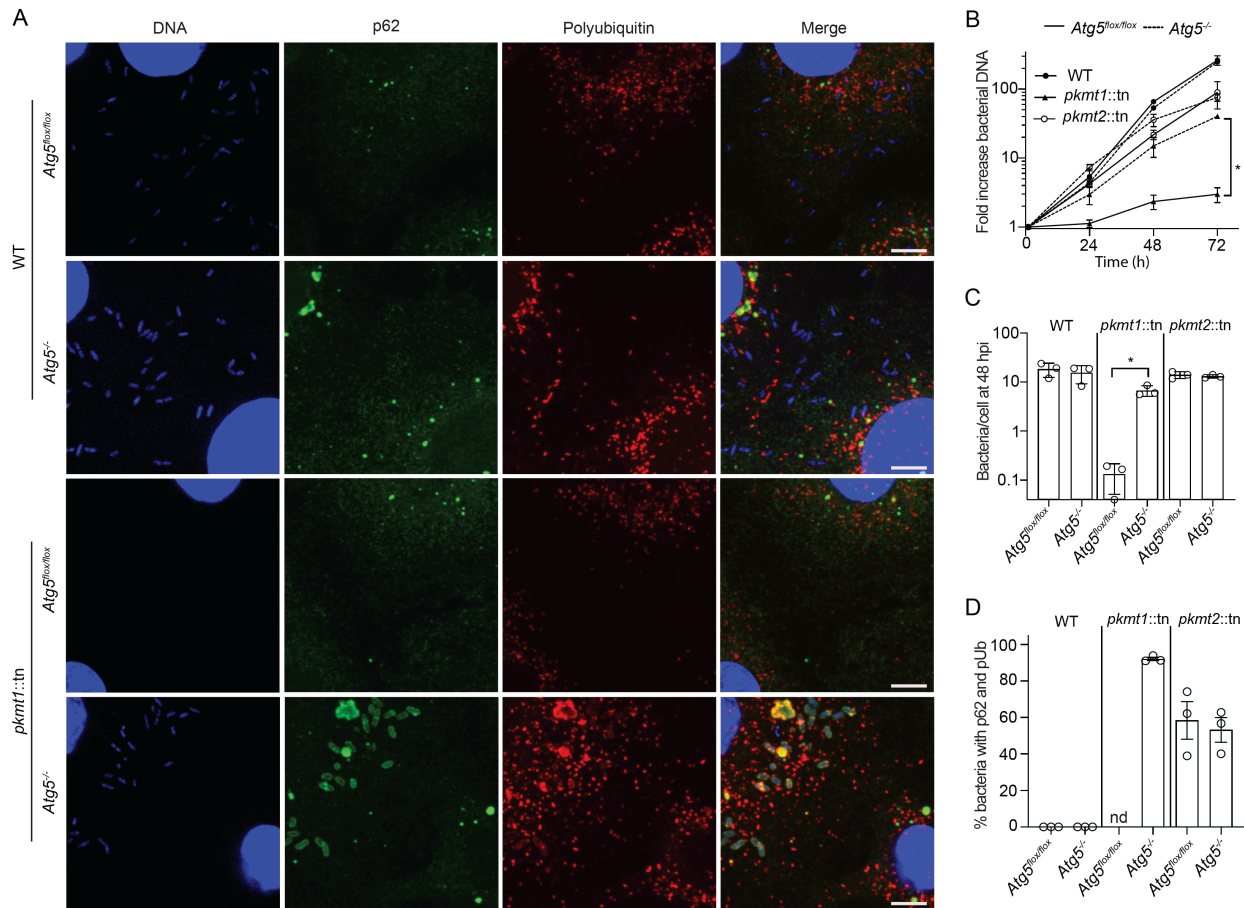
270

271 **Fig. 2. Lysine methylation protects OMPs from ubiquitylation.** (A) Micrographs of infected  
272 Vero cells expressing 6xHis-ubiquitin stained with anti-His antibody (red) and Hoechst (blue,  
273 bacterial and host DNA), at 28 h.p.i. Scale bar, 5  $\mu$ m (representative of  $n = 2$ ). (B) Western blot of  
274 His-Ub input and pull-down samples from infected control and 6xHis-ubiquitin expressing cells,  
275 probed for OmpB, OmpA, and pUb (representative of  $n = 3$ ). (C) pUb-enriched (TUBE-1, pan  
276 specific) samples from purified bacteria probed for OmpB, OmpA, and OmpW (OmpB and OmpA  
277 of endogenous molecular weight represent non-specific binding to TUBE-1 beads) (representative  
278 of  $n = 3$ ). Asterisks indicate OmpB and OmpA that exhibit increased molecular weight, indicating  
279 ubiquitylation. Arrows indicate OmpB and OmpA of endogenous molecular weight.



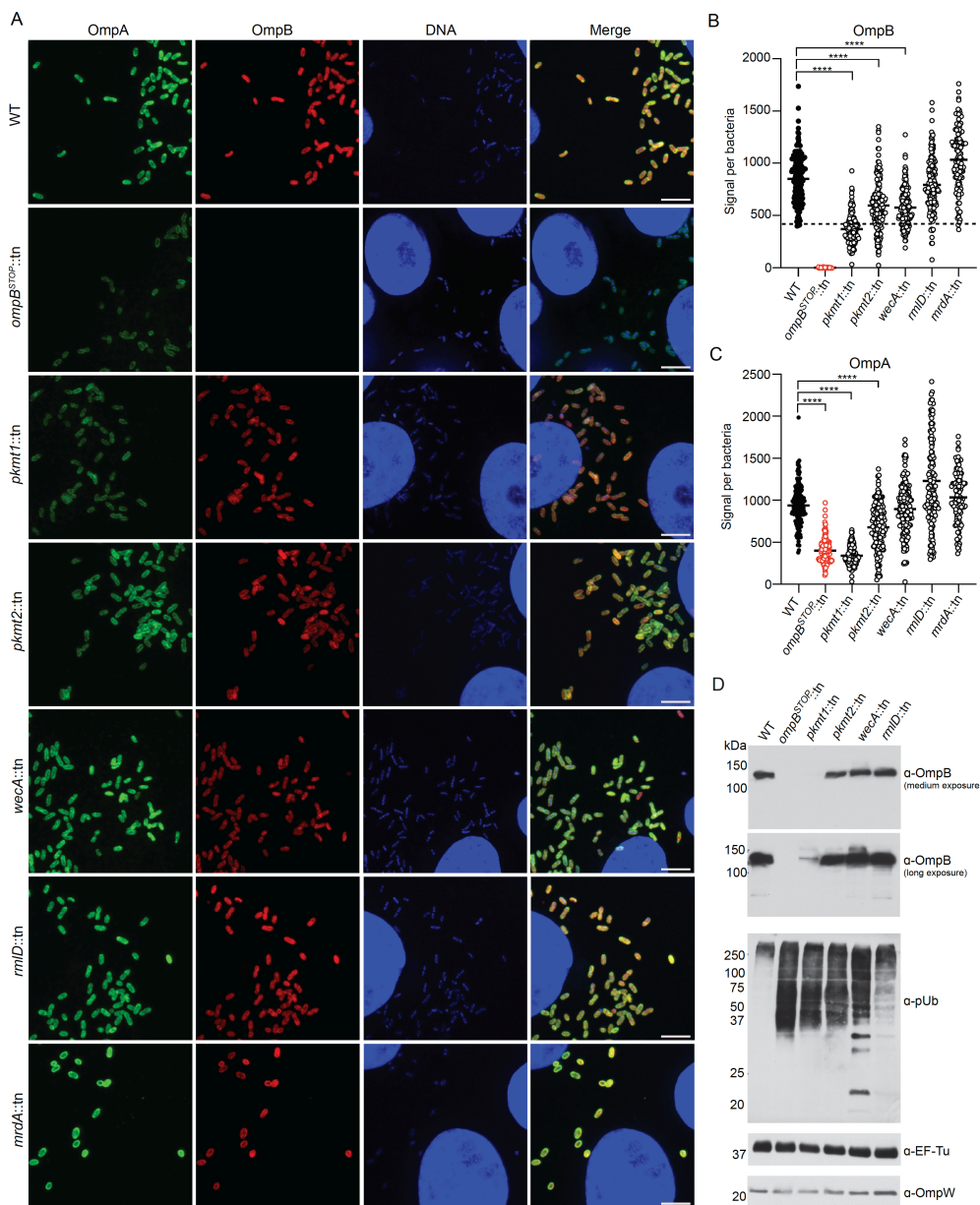
280

**Fig. 3. Methylation camouflages lysines from ubiquitylation.** (A) Percentage lysine methylation abundance of total among the abundantly detected proteins in WT *R. parkeri* determined by LC-MS (data are combined from  $n = 2$ ). (B) Methylated lysines (K) are indicated with residue number in each OMP, and lysines in *R. prowazekii* OmpB known to be methylated in green (17). K78, K131, K149, K312, and K547 in OmpB were unmethylated ( $n = 5$ , using data-independent and data-dependent acquisition modes). (C) Percentage of total abundances of the lysines methylated in B, that is unmethylated, mono-, di-, or tri-methylated (data are the mean of  $n = 2$ ). (D) Percentage of individual lysines in OmpB that are unmethylated, mono-, di- or tri-methylated. Only residues repeatedly detected in all strains were analyzed (data are the mean of  $n = 2$ ). (E) Heat map representation of OmpB residues from *pkmt1::tn* or *pkmt2::tn* that have similar levels of K-diGly peptides (white boxes) compared to WT, or with a 5-fold, or more, increase of K-diGly peptides (cyan) after pUb-enrichments ( $n = 2$ ). (F) Abundances of ubiquitylated (diGly), unmethylated, mono-, di-, or tri-methylated OmpB K623 (data are the mean of  $n = 2$ ). Each experiment ( $n$ ) was performed in technical triplicate.

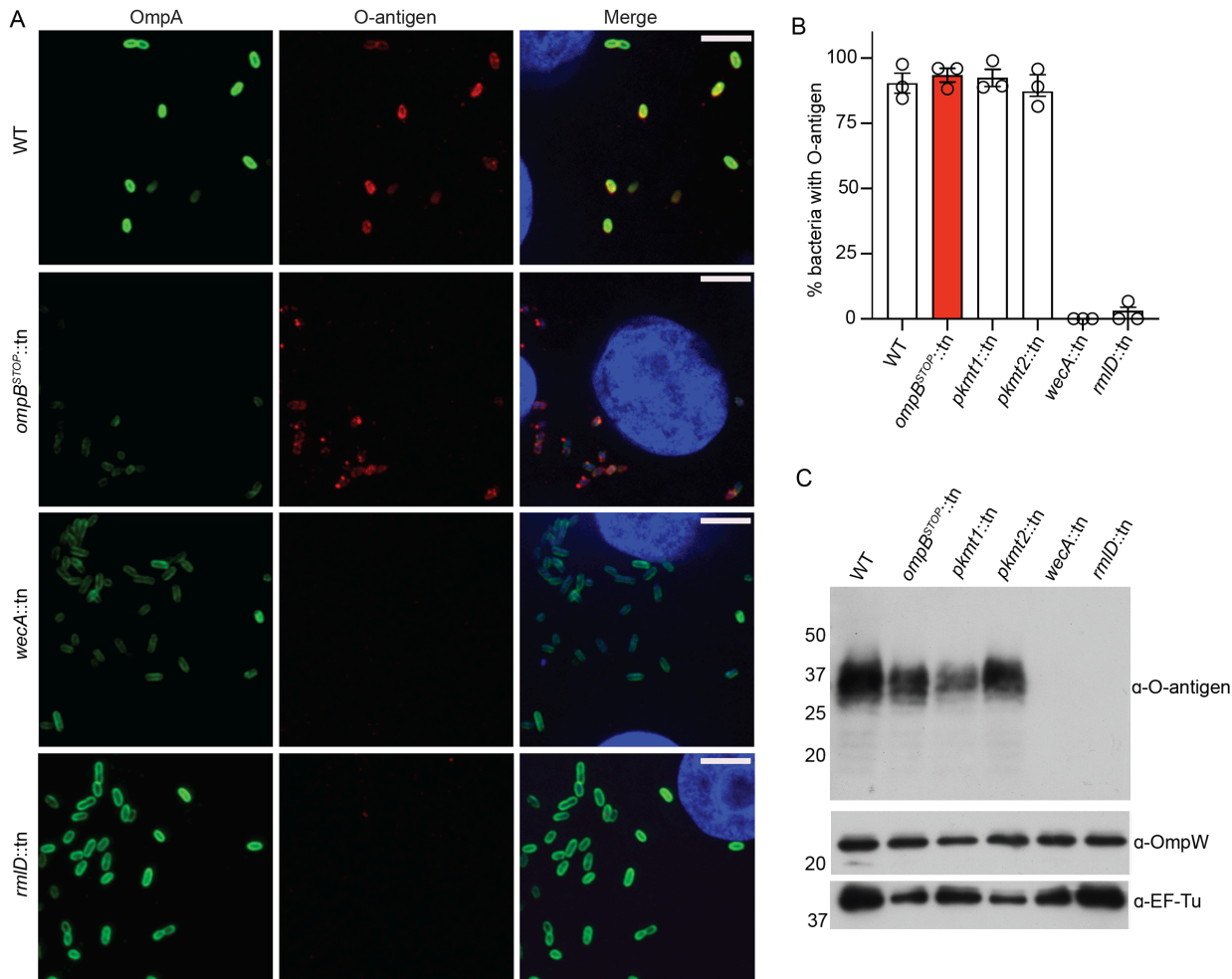


295  
296 **Fig. 4. Methylation prevents ATG5-dependent *R. parkeri* killing in macrophages. (A)**  
297 Micrographs of infected control (*Atg5*<sup>fl/fl</sup>) and *Atg5*-deficient (*Atg5*<sup>-/-</sup>) BMDMs at 48 h.p.i.,  
298 stained for DNA (blue), pUb (red), and p62 (green). Arrow indicate a bacterium positive for both  
299 pUb and p62. Scale bars, 5  $\mu$ m ( $n = 3$ ). (B) Bacterial growth curves in control and *Atg5*<sup>-/-</sup> BMDMs,  
300 as measured by genomic equivalents using qPCR ( $n = 3$ ). (C) Quantification of the mean number  
301 of bacteria per cell ( $n = 3$ ). (D) Quantification of the percentage of bacteria with p62 and pUb ( $n$   
302 = 3). nd, not determined. Statistical comparisons in **B** and **C** were performed using a Brown-  
303 Forsyth and Welch ANOVA with Dunnett's post-hoc test; \*,  $P < 0.05$ . Presented data are the mean  
304  $\pm$  s.e.m.  
305

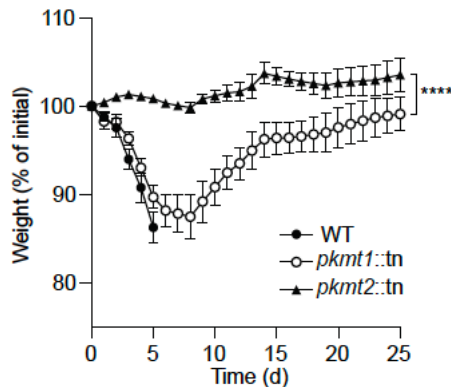
306 **Supplementary Figures**



307  
308 **Fig. S1. Polyubiquitylated mutant *R. parkeri* strains are positive for OmpA and OmpB. (A)**  
309 Micrographs of Vero cells infected with the indicated strains stained for OmpA (green, 13-3  
310 antibody), OmpB (red, OmpB-antibody), and DNA (blue, Hoechst) at 72 h.p.i. (representative of  
311  $n = 3$ ). Scale bar 5  $\mu$ m. **(B)** Quantification of OmpB signal per bacterium. (Lines indicate the means;  
312  $n = 3$  fields of vision;  $\geq 50$  bacteria per field of vision were analyzed). Statistical comparisons were  
313 performed using a Kruskal-Wallis test with Dunn's post-hoc test; \*\*\*\*  $P < 0.0001$  between  
314 indicated strains. Dashed line indicates that the majority of mutant bacterial populations, except  
315 *pkmt1::tn* bacteria, have OmpB levels comparable to WT bacteria. **(C)** Quantification of OmpA  
316 signal per bacterium as in **B**. **(D)** Western blot of  $5 \times 10^6$  purified bacteria probed for OmpB, pUb,  
317 OmpW and EF-Tu (bacterial loading controls) (representative of  $n = 2$ ).



318  
319 **Fig. S2. The *wecA::tn* and *rmlD::tn* bacteria lack the O-antigen. (A)** Micrographs of Vero cells  
320 infected with the indicated strains stained for OmpA (green, 13-3 antibody), the O-antigen (red,  
321 O-antigen antibody(15)) and DNA (blue, Hoechst) at 72 h.p.i. (representative of  $n = 3$ ). Scale bars,  
322 5  $\mu$ m. **(B)** Percentage of bacteria positive for the O-antigen at 72 h.p.i.  $n = 2$ ;  $\geq 90$  bacteria were  
323 counted in each infection (data are the mean  $\pm$  s.e.m.;  $n = 3$ ). **(C)** Western blot of  $5 \times 10^6$  purified  
324 WT and mutant bacteria probed for the O-antigen. OmpW and EF-Tu were used as bacterial  
325 loading controls (representative of  $n = 3$ ).



326

327 **Fig. S3. PKMT1 plays a more significant role in causing disease *in vivo* compared to PKMT2.**

328 (A) Weight changes of *Ifnar*<sup>-/-</sup>*Ifngr*<sup>-/-</sup> mice intravenous infected with 5x10<sup>6</sup> WT, *pkmt1::tn*, or  
329 *pkmt2::tn* bacteria (data are the mean  $\pm$  s.e.m.  $n = 5$ , WT;  $n = 6$ , *pkmt1::tn* and *pkmt2::tn*, combined  
330 from two independent experiments). A two-way ANOVA from 0 to 25 days post-infection (d.p.i.)  
331 was used to statistically compare the weight changes between the *pkmt1::tn* and *pkmt2::tn* mutants.  
332 \*\*\*  $P < 0.0001$ .

OMP-porin K-CH<sub>3</sub>(mono or di)

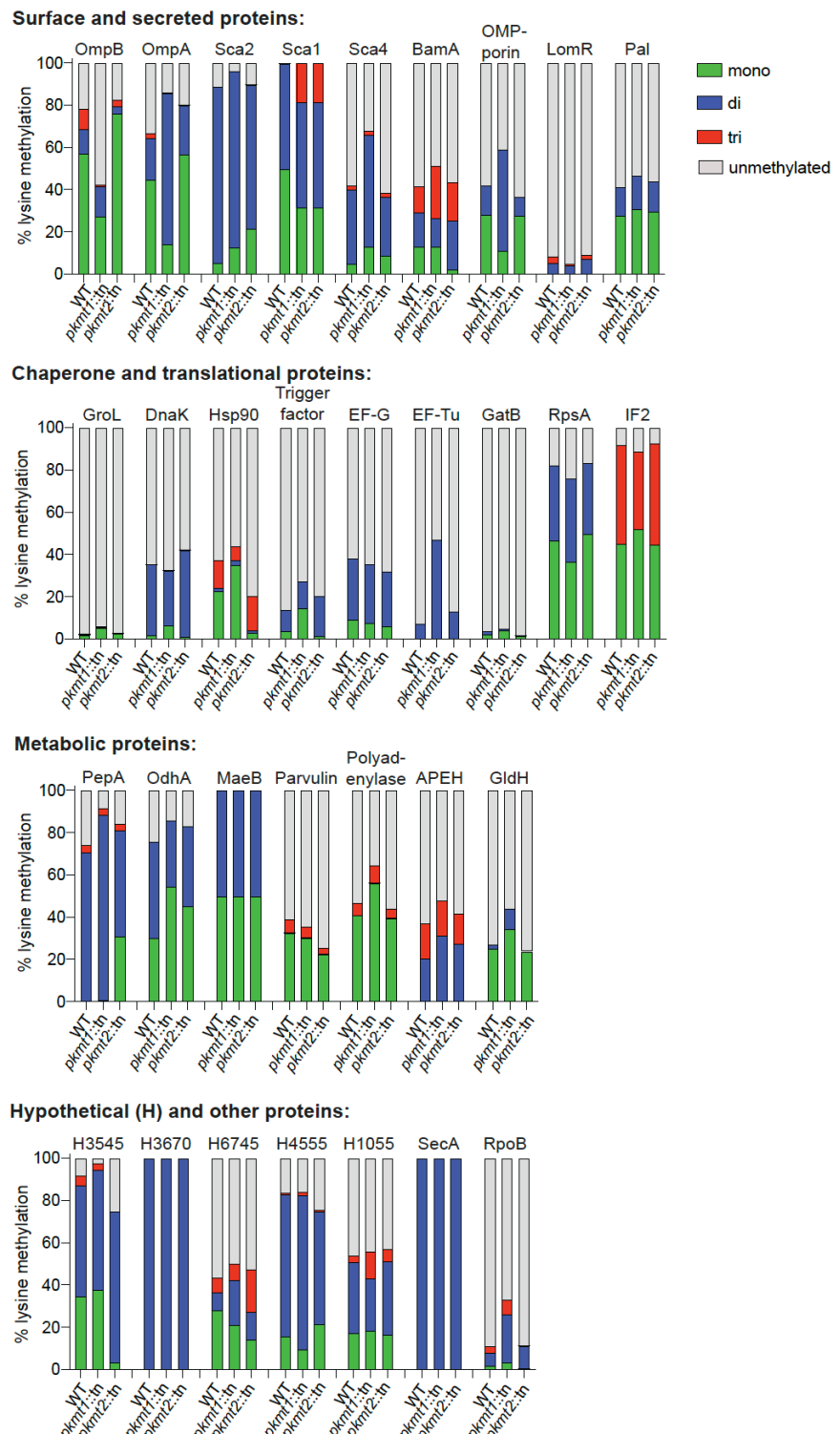
46	65	201	349	394	
1	K KK	K KK	KKKK	K K KKK K	438

### BamA K-CH<sub>3</sub>(mono or di)

51	205	287	408	420	597	772	770	768
1	K	K	K	KK	KKK	KKKK	KKKKK	KKKKKK

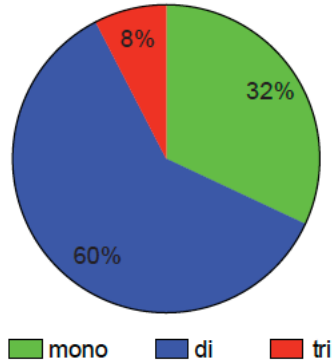
Sca4 -K-CH<sub>3</sub>(mono or di)

**Fig. S4. Lysine-methylome reveals that *R. parkeri* OMP-porin, BamA, and the released factor Sca4 are methylated.** Methylated lysines are indicated with residue number, and unmethylated residues without, determined by LC-MS as in **Fig. 3B** (data is combined from five independent experiments). See also **Table S2**.

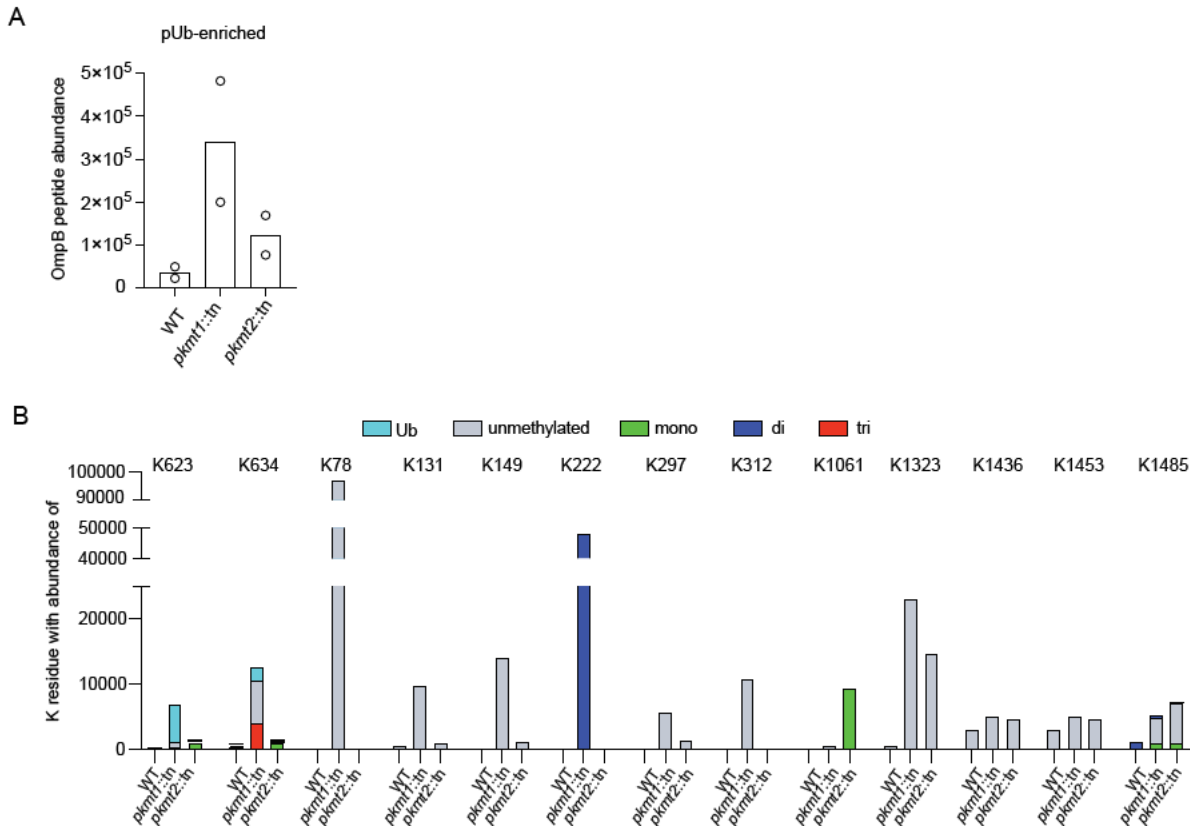


338

339 **Fig. S5. PKMT1 primarily modifies bacterial OMPs.** Percentage of total abundances of the  
340 lysines methylated in WT, that is unmethylated, mono-, di-, or tri-methylated in respective strain.  
341 Proteins with  $\geq 3$  lysines methylated detected in independent experiments are shown (mean of  $n =$   
342 2, performed in technical triplicates). OmpB, OmpA and Sca2 data are the same as in **Fig. 3C**. See  
343 also **Table S2**.

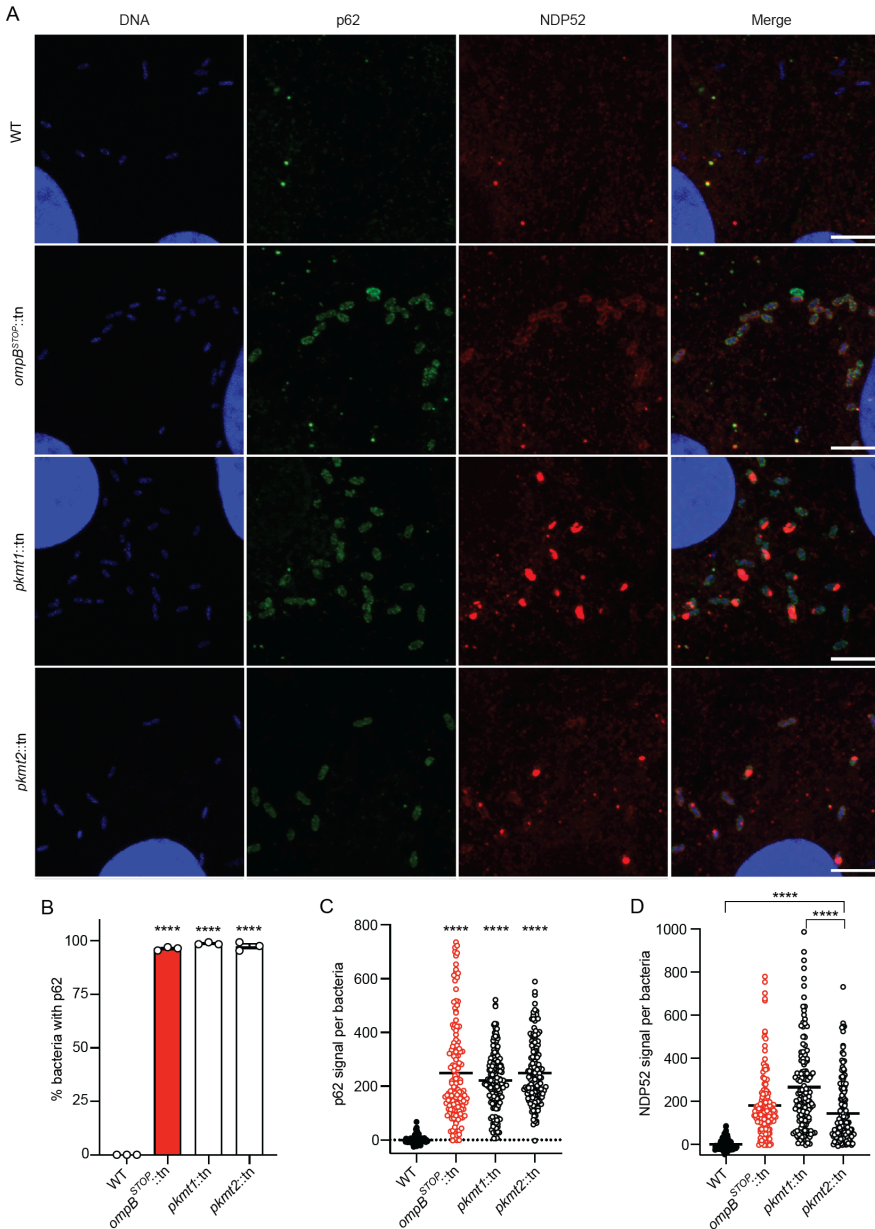


344  
345 **Fig. S6. Dimethylation is a common methylation state among the abundant *R. parkeri***  
346 **proteins.** Percentage of total lysines abundances detected to be mono-, di-, or tri-methylated in  
347 WT bacteria of the proteins indicated in **Table S2** (mean of  $n = 2$ , performed in technical  
348 triplicates).



349  
350  
351  
352  
353  
354  
355  
356

**Fig. S7. OmpB K623 and K634 are frequently ubiquitylated when PKMT1-mediated methylation is reduced.** (A) OmpB peptide abundance values after pUb-enrichments from respective strain, as determined by LC-MS (data are mean of  $n = 2$ , performed in triplicates). (B) Abundance values of lysines in OmpB that are ubiquitylated (diGly), unmethylated, mono-, di-, or tri-methylated, in respective strain after pUb-enrichments as in **Fig 2C**. Only residues detected in independent experiments are shown (data are the mean of  $n = 2$ , performed in technical triplicates). K623 data in **B** are the same as in **Fig. 3F**.



357

358

**Fig. S8. OmpB and lysine methylation block recruitment of autophagy receptors to *R. parkeri*.**

359 (A) Micrographs of Vero cells infected with the indicated strains: stained for bacterial and host DNA (blue, Hoechst), p62 (green, p62-antibody), and NDP52 (red, NDP52-antibody) at 72

360 h.p.i ( $n = 4$  for p62 staining;  $n = 2$  for NDP52 staining). (B) Percentage of bacteria that show rim- 361 like surface localization of p62 at 72 h.p.i. (Data are the mean  $\pm$  s.e.m.;  $n = 3$ ;  $\geq 142$  bacteria were 362 counted for each infection). Statistical comparisons between WT and *ompB<sup>STOP</sup>::tn*, *pkmt1::tn*, 363 *pkmt2::tn* were performed using a one-way ANOVA with Tukey's post-hoc test; \*\*\*\*  $P < 0.0001$ . 364 (C) Quantification of p62 signal per bacterium from a representative experiment. Lines indicate the 365 means. ( $n = 3$  fields of vision;  $\geq 50$  bacteria per field of vision were analyzed). Statistical 366 comparisons were performed using a Kruskal-Wallis test with Dunn's post-hoc test; \*\*\*\*  $P < 367 0.0001$  between indicated strains. (D) Quantification of NDP52 signal per bacteria as in C. 368

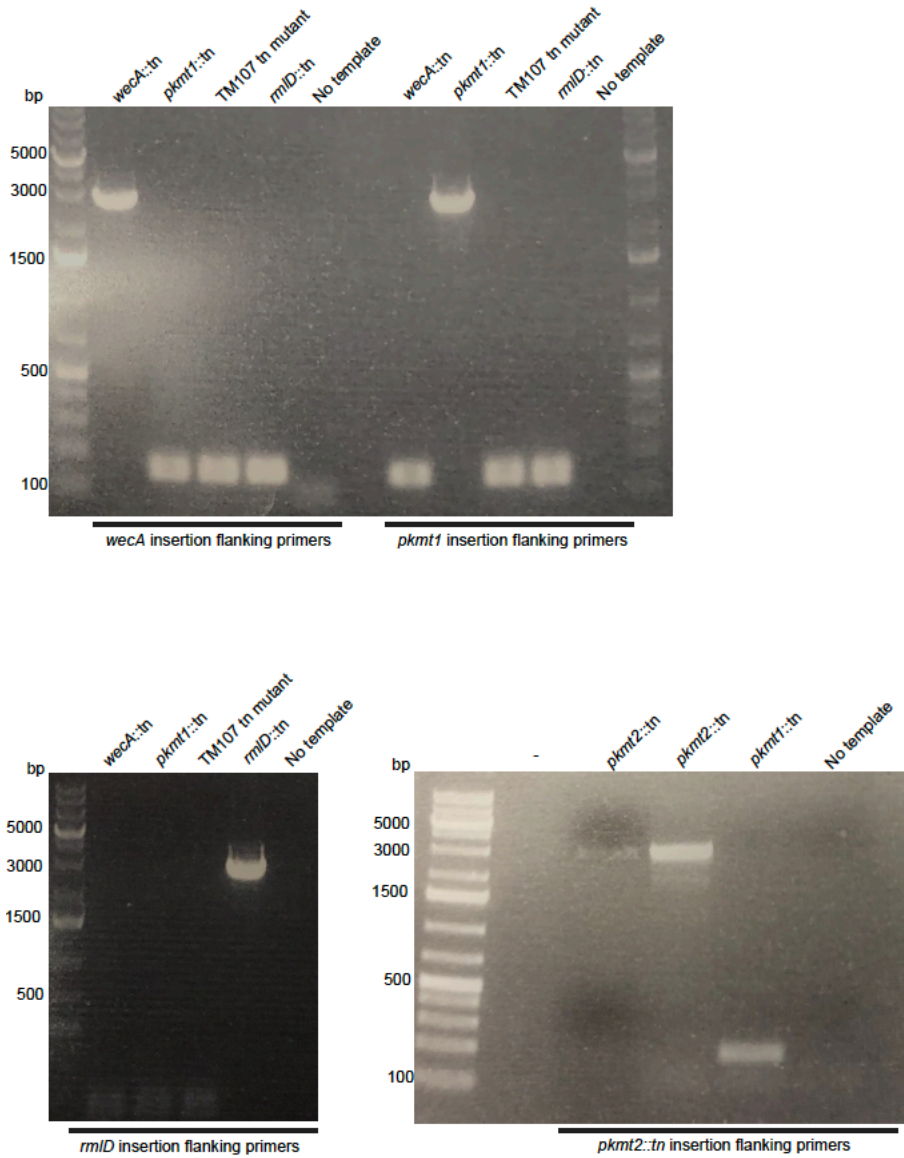
<i>Rickettsia parkeri</i>	1	MSPKVITNSSTPNGHDKMAKKTHSAQS VVN--GAVSDHNTYDEIPIYESYPYALTNPYHLSTLATLFGVNAPEVENAKILE	78
<i>Rickettsia rickettsii</i>	1	MSPKATNSSTPNGHDKMAKKTHSAQS VVN--GAVSDHNTYDEIPIYESYPYALTNPYHLSTLATLFGVNAPEVENAKILE	78
<i>Rickettsia conorii</i>	1	MSPKATNSSTPNGHDKMAKKTHSAQS VVN--GAVSDHNTYDEIPIYESYPYALTNPYHLSTLATLFGVNAPEVENAKILE	78
<i>Rickettsia typhi</i>	1	MSLKSSST----TNDHDK-TTKINSIQLVNctdTVADHNTYDEIPIYESYPYALTNPYHLSTLATLFGVNAPEVENAKILE	75
<i>Rickettsia prowazekii</i>	1	MSLKSTTSSLTTNNHDK-T--INSVQLVNgtGTVADHNTYDEIPIYESYPYALTNPYHLSTLATLFGVNAPEVENAKILE	77
<i>Rickettsia bellii</i>	1	MSAKASNSNLPNGHDKTKERNTQPVIN--GAIK-RNTYDEVYYESYPYSPTNFHLSTLATLFGVNAPEVENAKILE	77
<i>Rickettsia endosymbiont of Proechinophthirus fluctus</i>	1	MSPKATNSSTPNSHDKMAKKTHSVQS VVN--SAVSDHNTYDEIPIYESYPYAFTHPYHLSTLATLFGVNAPEVENAKILE	78
<i>Rickettsia parkeri</i>	79	LGCAAGGNLIPHAVLYPKAYFVGVDLSKVQIDEANKNVKALGLKNIEFHCSITDINDSFGKFDYIICHGVISWVPKTVR	158
<i>Rickettsia rickettsii</i>	79	LGCAAGGNLIPHAVLYPKAYFVGVDLSKVQIDEANKNVKALGLKNIEFHCSITDINDSFGKFDYIICHGVISWVPKTVR	158
<i>Rickettsia conorii</i>	79	LGCAAGGNLIPHAVLYPKAYFVGVDLSKVQIDEANKNVKALGLKNIEFHCSITDINDSFGKFDYIICHGVISWVPKTVR	158
<i>Rickettsia typhi</i>	76	LGCAAGGNLIPHAVLYPKAYFVGVDLSKVQIDEANKNVKALGLKNIEFHCSITDINDSFGKFDYIICHGVISWVPKIVR	155
<i>Rickettsia prowazekii</i>	78	LGCAAGGNLIPHAVLYPKAYFVGVDLSKVQIDEANKNVKALGLKNIEFHCSITDINDSFGKFDYIICHGVISWVPKIVR	157
<i>Rickettsia bellii</i>	78	LGCAAGGNLIPHAVLYPKAYFVGVDLSKVQIDEANKNVKALGLKNIEFHCSITDINDSLNKFDYIICHGVMSWVSKNVR	157
<i>Rickettsia endosymbiont of Proechinophthirus fluctus</i>	79	LGCAAGGNLIPHAVLYPKAYFVGVDLSKVQIDEANKNVKALGLKNIEFHCSITDINDSFGKFDYIICHGVISWVPKTVR	158
<i>Rickettsia parkeri</i>	159	DKIFEVCNKNLSPNGIAYISYNTLPGWNMVRTIRDMMYHSSSFANVRDRIAQSRLLLEFVKDSLSEN SKTPYAEALKTEA	238
<i>Rickettsia rickettsii</i>	159	DKIFEVCNKNLSPNGIAYISYNTLPGWNMVRTIRDMMYHSSSFANVRDRIAQSRLLLEFVKDSLSEN SKTPYAEALKTEA	238
<i>Rickettsia conorii</i>	159	DKIFEVCNKNLSPNGIAYISYNTLPGWNMVRTIRDMMYHSSSFANVRDRIAQSRLLLEFVKDSLSEN SKTPYAEALKTEA	238
<i>Rickettsia typhi</i>	156	DKIFVKVCNSNLSTNGIAYISYNTLPGWNMVRTIRDMMYHSSSFANVRDRIAQSRLLLEFVKDSLSEN SKTPYAEALKTEA	235
<i>Rickettsia prowazekii</i>	158	DKIFVKVCNRNLSTNGIAYISYNTLPGWNMVRTIRDMMYHSSSFANVRDRIAQSRLLLEFVKDSLSEN SKTPYAEALKTEA	237
<i>Rickettsia bellii</i>	158	DKIFDVVCNKNLSPNGIAYISYNTLPGWNMVRTIRDMMYHSSSFANVRDRIAQSRLLLEFVKDSLSEN SKTPYAEALKTEA	237
<i>Rickettsia endosymbiont of Proechinophthirus fluctus</i>	159	DKIFEVCNKNLSPNGIAYISYNTLPGWNMVRTIRDMMYHSSSFANVRDRIAQSRLLLEFVKDSLSEN SKTPYAEALKTEA	238
<i>Rickettsia parkeri</i>	239	GLLAQKTDHYLRDHLEEEAQFYFHEFMNEARKHNLQYIADCNLSTMLGNMPKVVQLKAVN DIVRTEQYMDFITNR	318
<i>Rickettsia rickettsii</i>	239	GLLAQKTDHYLRDHLEEEAQFYFHEFMNEARKHNLQYIADCNLSTMLGNMPKVVQLKAVN DIVRTEQYMDFITNR	318
<i>Rickettsia conorii</i>	239	GLLAQKTDHYLRDHLEEEAQFYFHEFMNEARKHNLQYIADCNLSTMLGNMPKVVQLKAVN DIVRTEQYMDFITNR	318
<i>Rickettsia typhi</i>	236	GLLAQKTDHYLRDHLEEEAQFYFHEFMNEARKYNLQYIADCNISTMLGNMPKVVQLKAVN DIVRTEQYMDFITNR	315
<i>Rickettsia prowazekii</i>	238	GLLAQKTDHYLRDHLEEEAQFYFHEFMNEARKHNLQYIADCNISTMLGNMPKVVQLKAVN DIVRTEQYMDFITNR	317
<i>Rickettsia bellii</i>	238	GLLSQTDQYFHLRDHLEEEAQFYFHEFMNEARKHNLQYIADCNISTMLGNMPKVVQLKAVN DIVRTEQYMDFITNR	317
<i>Rickettsia endosymbiont of Proechinophthirus fluctus</i>	239	GLLAQKTDHYLRDHLEEEAQFYFHEFMNEARKHNLQYIADCNLSTMLGNMPKVVQLKAVN DIVRTEQYMDFITNR	318
<i>Rickettsia parkeri</i>	319	RFRTTLLCHSDVKINRNINNDTITKFNIIIFNIVPEKPLKEVDLNNASENLKFFLNGNQDSNLTTSPYMKAILETFSEN	398
<i>Rickettsia rickettsii</i>	319	RFRTTLLCHSDVKINRNINNDTITKFNIIIFNIVPEKPLKEVDLNNASENLKFFLNGNQDSNLTTSPYMKAILETFSEN	398
<i>Rickettsia conorii</i>	319	RFRTTLLCHSDVKINRNINNDTITKFNIIIFNIVPEKPLKEVDLNNASENLKFFLNGNQDSNLTTSPYMKAILETFSEN	398
<i>Rickettsia typhi</i>	316	RFRTTLLCHNDLKLINRNINNEDITKFNIIIFNIVPEKPLKEVDLNNASENLKFFLNGNQDSNLTTSPYMKAILETFSEN	395
<i>Rickettsia prowazekii</i>	318	RFRTTLLCHNDLKLINRNINNDDITKFNIIIFNIVPEKPLKEVDLNNATENLQFFLNGNKECNLSTTSSPYMKAILETFSEN	397
<i>Rickettsia bellii</i>	318	RFRSTLLCHNDVVKINRNINNEDIMKFNIFNVVPEKSLEVKDLNNASSESLAFFLNGNQDSNLTTSPYMKAILETFSEN	397
<i>Rickettsia endosymbiont of Proechinophthirus fluctus</i>	319	RFRTTLLCHSDVKINRNINNDTITKFNIIIFNIVPEKPLKEVDLNNASENLKFFLNGNQDSNLTTSPYMKAILETFSEN	398
<i>Rickettsia parkeri</i>	399	NNPLSFEKITTEANKKLHNTKLNEIKAELNNAMKLVLQGYISITNQKHNPNPELDKPKTTKMVIHQATHTPSMWVTLNK	478
<i>Rickettsia rickettsii</i>	399	NNPLSFEKITTEANKKLHNTKLNEIKAELNNAMKLVLQGYISITNQKHNPNPELDKPKTTKMVIHQATHTPSMWVTLNK	478
<i>Rickettsia conorii</i>	399	NNPLSFEKITTEANKKLHNTKLNEIKAELNNAMKLVLQGYISITNQKHNPNPELDKPKTTKMVIHQATHTPSMWVTLNK	478
<i>Rickettsia typhi</i>	396	NNPLSFKQVTSEANKKLNNNKLNEIKAELLNAMKLVLQGYISITNQKHNPKVFLDKPKTTQVLYQAKHTPSMWVTLNK	475
<i>Rickettsia prowazekii</i>	398	NNPLSFRQVTSEANKKLNNNKLNEIKAELLNAMKLVLQGYISITNQKHNPKVFLDKPKTTQVLYQAKHTPSMWVTLNK	477
<i>Rickettsia bellii</i>	398	NNPLSFEKITEEANKKLHGTKLNEIKAELLNAMKLVLQGYIN1TTQKHRETPELNPKPTTKLVHQIAHTPYMWVTLNK	477
<i>Rickettsia endosymbiont of Proechinophthirus fluctus</i>	399	NNPLSFEKITTEANKKLHNTKLNEIKAELLNAMKLVLQGYISITNQKHNPNPELDKPKTTKMVIHQATHTPSMWVTLNK	478
<i>Rickettsia parkeri</i>	479	HEPIGVNFFEKFAFLRYMDGKHDKKAIAEVLGHVKEGELTLSKEQGVKENKEIRKELESLFPIPMIKKFSSNALLV	554
<i>Rickettsia rickettsii</i>	479	HEPIGVNFFEKFAFLRYMDGKHDKKAIAEVLGHVKEGELTLSKEQGVKENKEIRKELESLFPIPMIKKFSSNALLV	554
<i>Rickettsia conorii</i>	479	HEPIGVNFFEKFAFLRYMDGKHDKKAIAEVLGHVKEGELTLSKEQGVKENKEIRKELESLFPIPMIKKFSSNALLV	554
<i>Rickettsia typhi</i>	476	HEPIGVNFFEKFAFLRYMDGKNDKKAIAEVLGHVKEGELTLSKEQGVKENKEIRKELESLFPIPMIKKFSSNALLV	551
<i>Rickettsia prowazekii</i>	478	HEPIGVNFFEKFAFLRYMDGRNDKKAIAEVLGHVKEGELTLSREGQKIEENKEIRKELESLFPIPMIEKFCSNALLV	553
<i>Rickettsia bellii</i>	478	HEPVGVNFFEKLAIRYMDGKHDKKAIAEVLGHVKEGELTLSKGQKIEEDQEVIRKQLEVLFPMPMIDKFAANALLV	553
<i>Rickettsia endosymbiont of Proechinophthirus fluctus</i>	479	HEPIGVNFFEKFAFLRYMDGKHDKKAIAEVLGHVKEGELTLSKGQKIEEDQEVIRKQLEVLFPMPMIDKFAANALLV	554

369 **Fig. S9. The PKMT1 enzyme is highly conserved between diverse rickettsial species.** Amino  
 370 acid sequence alignment of PKMT1 from *R. parkeri* ([WP\\_014411082.1](https://www.uniprot.org/uniprot/WP_014411082.1)), *R. rickettsii*  
 371 ([WP\\_012262600.1](https://www.uniprot.org/uniprot/WP_012262600.1)), *R. conorii* ([WP\\_016926592.1](https://www.uniprot.org/uniprot/WP_016926592.1)), *R. typhi* ([WP\\_011191207.1](https://www.uniprot.org/uniprot/WP_011191207.1)), *R. prowazekii*  
 372 ([WP\\_004596928.1](https://www.uniprot.org/uniprot/WP_004596928.1)), *R. bellii* ([WP\\_045799810.1](https://www.uniprot.org/uniprot/WP_045799810.1)), and a *Rickettsia* endosymbiont  
 373 ([WP\\_062811822.1](https://www.uniprot.org/uniprot/WP_062811822.1)), using **COBALT**. Amino acids indicated in red are identical; blue, variation  
 374 between species; grey, one or more of the analyzed proteins are lacking this residue(s).

<i>Rickettsia parkeri</i>	1	MTKQANKISYDEVYPSPFTFSYTSPPYLRTIGKLFGLNPPLAKILELGCIGIVNLLNFAETYPKSQSLGVDSLSTQI	80
<i>Rickettsia rickettsii</i>	1	MTKQANKISYDEVYPSPFTFSYTSPPYLRTIGKLFGLNPPLAKILELGCIGIVNLLNFAETYPKSQSLGVDSLSTQI	80
<i>Rickettsia conorii</i>	1	MTKQANKISYDEVYPSPFTFSYTSPPYLRTIGKLFGLNPPLAKILELGCIGIVNLLNFAETYPKSQSLGVDSLSTQI	80
<i>Rickettsia typhi</i>	1	MIKKANKISYDEVYPYPPTFSYTYPYPLRTIGKLFGLNPPLAKILELGCIGIVNLLNFAETYPKSQSLGVDSLSTQI	80
<i>Rickettsia prowazekii</i>	1	MIKTKNKISYDEVYPYPPTFSYTYPYPLRTIGKLFGLNPPLAKILELGCIGIVNLLNFAETYPKSQSLGVDSLSTQI	80
<i>Rickettsia parkeri</i>	81	ELGKKFISDLKIKNAELKALSIIDLDESYGKFDYIVCHGVYSWVPEEVQDKILKVCNKLLNPNGIAFVSYNTLPGWNMQR	160
<i>Rickettsia rickettsii</i>	81	ELGKKIISDLKIKNAELKALSIIDLDESYGKFDYIICHGVYSWVPEEVQDKILKVCNKLLNPNGIAFVSYNTLPGWNMQS	160
<i>Rickettsia conorii</i>	81	ELGKKIISDLKIKNAELKALSIIDLDESYGKFDYIVCHGVYSWVPEEVQDKILKICNKLLNPNGIAFVSYNTLPGWNMQR	160
<i>Rickettsia typhi</i>	81	ELGKKTISDAKINNVELKALSIIDLDESYGKFDYIVCHGVYSWVSEVQDKILEVLNKLLNPNGIAFVSYNTLPGWNMQN	160
<i>Rickettsia prowazekii</i>	81	BIGKKTISDSKIKNVGLKALSIIDLDESYGKFDYIVCHGVYSWVSEVQDKILEVLNKLLNPNGIAFVSYNTLPGWNMQN	160
<i>Rickettsia parkeri</i>	161	TIREMIMFHSELFNTSHDKLQQAKLLLKFINDSLESSTTPYSNFLRDETKLLSAYTDSYVLHEYLGEINTGIFYHQFIEK	240
<i>Rickettsia rickettsii</i>	161	TIREMIMFHSELFNTSHDKLQQAKLLLKFINDSLESSTTPYSNFLRDETKLLSAYTDSYVLHEYLGEINTGIFYHQFIEK	240
<i>Rickettsia conorii</i>	161	TIREMIMFHSELFNTSHDKLQQAKLLLKFINDSLESSTTPYSNFLRDETKLLSAYTDSYVLHEYLGEINTGIFYHQFIEK	240
<i>Rickettsia typhi</i>	161	TIREMMMFHSESFNTSHDKLQQARLLLKFINDSLGNSTTPYANFLRDEAKLISTRYDDSYVLHEYLGEINTGTYHQFIEK	240
<i>Rickettsia prowazekii</i>	161	TIREMMMFHSESFNTSHDKLQQSKLLLKFINDSLENSTTPYANFLREEAKLISTRYADSYVLHEYLGEINTGTYHQFIEK	240
<i>Rickettsia parkeri</i>	241	AQKHNHLNYLGDTSLTAMPIGNLPTQAAEKLQAVNDIVRTEQYMDFITNRKFRSTLLCHQNIPINRKIEFNNLKEFFTSLN	320
<i>Rickettsia rickettsii</i>	241	AQKHNHLNYLGDTSLTAMPIGNLPTQAAEKLQAVNDIVRTEQYMDFITNRKFRSTLLCHQNIPINRKIEFNNLKEFFTSLN	320
<i>Rickettsia conorii</i>	241	AQKHNHLNYLGDTSLTAMPIGNLPTQAAEKLQAVNDIVRTEQYMDFITNRKFRSTLLCHQNIPINRKIEFNNLKEFFTSLN	320
<i>Rickettsia typhi</i>	241	AQKHNHLNYLGDTSAIAMFIGNLPTKAASKLQAIINDIVCTEQYMDFITNRKFRSTLLCHQNIPINRKIEFDNLKDFYTFN	320
<i>Rickettsia prowazekii</i>	241	AQKHNHLNYLGDTSAITAMPIGNLPTKAASKLQAIINDIVRTEQYMDFITNRKFRSTLLCHQNIPINRKIEFENLKDFTTFN	320
<i>Rickettsia parkeri</i>	321	IRPVILEKAVDLTNEQENVGFYYENLPEPFISTTSPIMKAILLYVVAENIGNPISLEQVAKAEFKKLGKYQLQDFLALEQ	400
<i>Rickettsia rickettsii</i>	321	IRPVILEKAVDLTNEQENVSFYYENLPEPFISTTSPIMKAILLYVVAENISNPISLEQVAKAEFKKLGKYQLQDFLALEQ	400
<i>Rickettsia conorii</i>	321	IRPVILEKAVDLTNEQENVSFYYENLPEPFISTTSPIMKAILLYVVAENISNPISLEQVAKAEFKKLGKYQLQDFLALEQ	400
<i>Rickettsia typhi</i>	321	IRPISPEKIDLNNEQENISFYENLPEPFISTTSAIMKAILLYVVAENISNPIRLEQVAKAEFKKLGKYRLQDFLATLEQ	400
<i>Rickettsia prowazekii</i>	321	IRPISENKIDLNNEQENISFYENLPEPFISTTSAIMKAILLYVVAENISNPIRLEQVAKAEFKKLGKYQLQDFLALEQ	400
<i>Rickettsia parkeri</i>	401	HFIIFIFQGYLKIFETKPHAIATITEKPKTSEFARYQAKQAYFNNVTSVFSVTNRLNDMVGIPIFIHEKYILEMLDGTHNID	480
<i>Rickettsia rickettsii</i>	401	HFIIFIFQGYLKIFETKPHAIATITEKPKTSEFARYQAKQAYFNNVTSVFSVTNRLNDMVGIPIFIHEKYILEMLDGTHNID	480
<i>Rickettsia conorii</i>	401	HFIIFIFQGYLKIFETKPHAIATITEKPKTSEFARYQAKQAYFNNVTSVFSVTNRLNDMVGIPIFIHEKYILEMLDGTHNID	480
<i>Rickettsia typhi</i>	401	HFITLIFQGYLKIFETKPHAIATITEKPKTSQFARYQAKAHFNNVTNMFSITNRLNDMIGIPIHEKYILEMLDGTHNID	480
<i>Rickettsia prowazekii</i>	401	HFITFIFQGYLKIFETKPHAIATITEKPKTSQFVRYQAKAHFNNVTNMLSVTNRLNDMIGIPIHEKYILEMLDGTHNID	480
<i>Rickettsia parkeri</i>	481	DIKKGVLEKINSKLLTARDDKQEVTDPKLLKEFVDYVVNTSLEKFRINYLVE	534
<i>Rickettsia rickettsii</i>	481	DIKKGVLEKINSKLLTARDDKQEVTDPKLLKEFVDYAVNTSLEKFRINYLVE	534
<i>Rickettsia conorii</i>	481	DIKKGVLEKINSKLLTARDDKQEVTDPKLLKEFVDYVVNTSLEKFRINYLVE	534
<i>Rickettsia typhi</i>	481	DIKKSIIEKINSKLLTACDNKGQVVTDPKLLKEFVDYVVAVSLEKFRINYLVE	534
<i>Rickettsia prowazekii</i>	481	DIKKGMIEKINSKLLIACDNKGQAVTDPKLLKEFVDYIVNISLEKFRINYLIG	534

376

377 **Fig. S10. The PKMT2 enzyme is highly conserved between virulent rickettsial species but**  
 378 **absent from *R. bellii* and the *Rickettsia endosymbiont Proechinophthirus fluctus*.** Amino acid  
 379 sequence alignment of PKMT2 from *R. parkeri* ([WP\\_014410272.1](#)), *R. rickettsii*  
 380 ([WP\\_012150259.1](#)), *R. conorii* ([WP\\_016925880.1](#)), *R. typhi* ([WP\\_011190574.1](#)), and *R.*  
 381 *prowazekii* ([WP\\_004596662.1](#)) using **COBALT**. PKMT1 of *R. bellii* and the *Rickettsia*  
 382 *endosymbiont Proechinophthirus fluctus* showed 51% identity to PKMT2 of *R. parkeri* using  
 383 single alignment BLAST at NCBI; however, no PKMT2 variants could be found in these  
 384 organisms, and therefore they were excluded from this analysis. Amino acids indicated in red are  
 385 identical; blue, variation between species.



386

387

388 **Fig. S11.** Strain validation of clonality and insertion site using primers for flanking chromosomal regions ( $n = 1$ ).

389 **Materials and Methods**

390 **Cell lines and primary mouse macrophages**

391 Vero cells were purchased from the UC Berkeley Cell Culture Facility and the identity was  
392 repeatedly confirmed by mass-spectrometry analysis. Cells were grown at 37 °C and 5% CO<sub>2</sub> in  
393 DMEM (Gibco, cat. no. 11965) with high glucose (4.5 g l<sup>-1</sup>) and 2% heat-inactivated (30 min, 56  
394 °C, in a water-bath) fetal bovine serum (Gemcell). Vero cells were confirmed to be mycoplasma  
395 negative by DAPI staining and fluorescence microscopy screening at the UC Berkeley Cell Culture  
396 Facility.

397 BMDMs generated from the femurs of mutant *Atg5*<sup>fl/fl</sup> and matched *Atg5*<sup>-/-</sup> C57BL/6  
398 mice were a kind gift from the laboratory of Jeffery S. Cox (UC Berkeley), and they were prepared  
399 as previously described (11) although in the absence of antibiotics. Genotypes were confirmed by  
400 PCR and Sanger sequencing at the UC Berkeley DNA Sequencing Facility, as previously  
401 described (11).

402

403 ***Rickettsia parkeri* strain generation and validation**

404 WT *R. parkeri* strain Portsmouth (NCBI accession no. [NC\\_017044.1](#); originally a gift from  
405 C. Paddock, Center for Disease Control and Prevention) and bacterial stocks of *ompB*<sup>STOP</sup>::tn (the  
406 genome sequences of these bacterial strains are available at the Sequence Read Archive as  
407 accession no. [SRP154218](#) (WT, [SRX4401164](#); *ompB*<sup>STOP</sup>::tn, [SRX4401167](#)), *pkmt1*::tn,  
408 *pkmt2*::tn, *wecA*::tn and *rlmD*::tn mutants were propagated and purified every ~6-10 months as  
409 described below. Side-by-side experimental comparisons were made between stocks prepared at  
410 similar times.

411 *R. parkeri* *pkmt1*::tn, *pkmt2*::tn, *wecA*::tn, and 114 other transposon insertion mutant

412 strains, screened for pUb, were previously isolated in a screen for small plaque mutants (13, 22).  
413 The *ompB<sup>STOP</sup>::tn* was previously isolated in a suppressor screen and lacked expression of OmpB  
414 (11). The *rmlD::tn*, and 132 other transposon insertion mutant strains, screened for pUb, were  
415 isolated in an independent screen in which mutants were isolated without regard for plaque size  
416 (**Table S1**). The genomic locations of transposon insertion sites for all mutants were determined  
417 by semi-random nested PCR. To verify the insertions and clonality, we used PCR reactions that  
418 amplified the transposon insertion site using primers for flanking chromosomal regions:  
419 5'GCTCACTAGATAGCACTCG'3 and 5'GCTCGATTATCTCACTTATG'3 for *rmlD::tn*,  
420 5'CGTTAATAGTCCAGTTAATTGT'3 and 5'CCGTCTATACCGTCCATAAAAT'3 for  
421 *wecA::tn*, 5'GCATCGAAATAACCCTGAG'3 and 5'GCAAACCTCTCAAAGAAATTAACG'3  
422 for *pkmt1::tn*, 5'GCTAAGAAATCTTCTAATTGATATTTAC'3 and  
423 5'CGAAAATTACCTGAGCCTT'3 for *pkmt2::tn*, 5'CGACACATAATAGCACAAACTAC'3  
424 and 5'GC GGAGGCGGTAGTAAAG'3 for *mrdA::tn* (**Fig. S11**).  
425

## 426 Screening for pUb-positive strains

427 To prepare the mutant library for screening, passage 1 (P1) transposon insertion mutants  
428 were amplified one time in Vero cells using 24-well cell culture plates. At 5-12 d.p.i, when 50-  
429 70% of the infected cells appeared to be rounded up (as a sign of infection) by visual inspection  
430 using a light microscope, cell culture media were completely removed, and cells were subsequently  
431 lysed in 500  $\mu$ L cold sterile water for 2-3 minutes (min). Next, 500  $\mu$ L of 2x cold sterile brain-  
432 heart-infusion (BHI) broth (BD Difco, 237500) was added to the lysed cells, resuspended, and P2  
433 bacteria were transferred to cryogenic storage vials and frozen at -80 °C.

434 To screen for pUb-positive strains, 10-40  $\mu$ L of each of five to seven P2 mutant bacterial  
435 strains were diluted in 1 mL of room temperature (RT) cell culture media supplemented with 2%  
436 FBS. Subsequently, the pooled bacterial suspension was centrifuged at 250g for 4 min at RT onto  
437 confluent Vero cells grown on coverslips in 24-well plates. Cells were then incubated at 33 °C and  
438 fixed at 50-55 h.p.i. with pre-warmed 4% paraformaldehyde (PFA) (Ted Pella Inc., 18505) for 10  
439 min at RT. If cells were over-infected (i.e., individual infection foci had grown together) as  
440 determined by immunofluorescence microscopy, infections of that specific pool were repeated  
441 using reduced volumes of P2 bacteria. Next, fixed cells were permeabilized with 0.2% Triton-X  
442 for 5 min and then stained with the anti-*Rickettsia* I7205 antibody (1:500 dilution; gift from Ted  
443 Hackstadt) and anti-polyubiquitin FK1 antibody (Enzo Life Sciences, BML-PW8805-0500; 1:250  
444 dilution), followed by Alexa 488 anti-rabbit antibody (Invitrogen, A11008; 1:500 dilution) or goat  
445 anti-mouse Alexa-568 (Invitrogen, A11004). Whole coverslips were manually inspected on a  
446 Nikon Ti Eclipse microscope with 60x (1.4 numerical aperture) Plan Apo objective. The initial  
447 screen revealed that five out of 39 mutant pools contained pUb-positive areas.

448 In a secondary screen, individual strains from the pUb-positive pools were used to infect  
449 Vero cells, as stated above. Infected cells were also fixed and stained as above except that a post-  
450 fixation step using 100% methanol for 5 min was included and an OmpB antibody (11) and  
451 Hoechst (Sigma, B2261, 1:2500 dilution) was used instead of the anti-*Rickettsia* I7205 antibody.  
452 Samples were inspected as above and strains were scored as follows: 1) pUb-negative (49 strains),  
453 2) a few infection foci were pUb-positive (2 strains: Sp mutant 24, insertion at bp position 753916;  
454 Sp mutant 94, insertion at bp position 774831), 3) bacteria in the center of foci were pUb-positive  
455 but not on the edges (2 strains: Sp mutant 43, insertion at bp position 651602-651604; Sp mutant  
456 45, insertion at bp position 751156), 4) almost all bacteria in all foci were pUb-positive (4 strains):

457 *pkmt1*::tn, insertion at bp position 1161553 (gene *MC1\_RS06185*); *pkmt2*::tn, insertion at bp  
458 position 34100 (*MC1\_RS00180*); *wecA*::tn, insertion at bp position 1223170 (*MC1\_RS06510*); and  
459 *rmlD*::tn, insertion at bp position 455753 (*MC1\_RS02345*).

460

461 ***Rickettsia* purification**

462 *R. parkeri* strains were propagated as described previously (11). “Purified bacteria” were  
463 from five T175 flasks of Vero cells that after 5-8 days of infection (normally ~75% infected as  
464 observed by light microscopy) were harvested in the media using a cell scraper. Bacteria were then  
465 centrifuged 12000g for 15 min at 4 °C in pre-chilled tubes. Pellets were resuspended in cold K-36  
466 buffer (0.05 M KH<sub>2</sub>PO<sub>4</sub>, 0.05 M K<sub>2</sub>HPO<sub>4</sub>, pH 7, 100 mM KCl and 15 mM NaCl) and a pre-chilled  
467 dounce-homogenizer (tight fit) were used for 60 strokes to release bacteria from host cells. The  
468 homogenate was then centrifuged at 200g for 5 min at 4 °C to remove cellular debris. The  
469 supernatant was overlaid onto cold 30% v/v MD-76R (Mallinckrodt Inc., 1317-07) diluted in K-  
470 36, and centrifuged at 58300g for 20 min at 4 °C in an SW-28 swinging-bucket rotor. The bacterial  
471 pellet was resuspended in cold 1x BHI broth (0.5 mL BHI per infected T175 flask), and after letting  
472 DNA precipitates sediment to the bottom of the tubes, bacterial suspensions were collected,  
473 aliquoted and frozen at -80 °C.

474 “Gradient-purified bacteria” were from ten T175 flasks of Vero cells, purified as above  
475 with the addition of a 40/44/54% v/v MD-76R (diluted in K-36 buffer) gradient step centrifuged  
476 at 58300g for 25 min at 4 °C using the SW-28 swinging bucket rotor. The bacteria were then  
477 collected from the 44-54% interface, diluted in K-36 buffer, and pelleted by centrifugation at  
478 12000g for 15 min at 4 °C. The pellet was resuspended in cold 1x BHI broth and subsequently  
479 aliquoted and frozen at -80 °C.

480

481 **OmpW and EF-Tu antibody production**

482 The sequence encoding amino acids 22-224 of outer membrane protein W (OmpW;  
483 WP\_014411122.1) (a protein that lacks the signal peptide), or full-length Elongation factor Tu  
484 (EF-Tu; WP\_004997779.1), were amplified by PCR from *R. parkeri* genomic DNA, and  
485 subsequently cloned into plasmid pETM1, which encodes N-terminal 6xHis and maltose-binding  
486 proteins (MBP) tags. From the resulting plasmids, fusion proteins were expressed in *E. coli* strain  
487 BL21 codon plus RIL-Cam<sup>r</sup> (DE3) (QB3 Macrolab, UC Berkeley) by induction with 1 mM  
488 isopropyl- $\beta$ -D-thio-galactoside (IPTG) for 2-2.5 hours at 37 °C. Bacterial pellets were resuspended  
489 in lysis buffer (50 mM NaH<sub>2</sub>PO<sub>4</sub>, pH 8.0, 300 mM NaCl, 1mM EDTA, and 1 mM dithiothreitol  
490 (DTT)) and stored at -80 °C. For protein purification, bacteria were thawed, lysozyme was added  
491 to 1 mg/mL (Sigma, L4919), and lysis was carried out by sonication. Lysates containing 6xHis-  
492 MBP-OmpW and 6xHis-MBP-EF-Tu were incubated on amylose resin (New England Biolabs,  
493 E8021L) (Qiagen, 1018244) and bound proteins were eluted in lysis buffer lacking EDTA and  
494 DTT but containing 10 mM maltose. Fractions were analyzed by SDS-PAGE and those with the  
495 highest concentrations of fusion proteins were pooled to generate rabbit antibodies against OmpW  
496 and EF-Tu. 1.2 mg of purified 6xHis-MBP-OmpW and 6xHis-MBP-EF-Tu proteins were sent to  
497 Pocono Rabbit Farm and Laboratory (Canadensis, PA), and immunization was carried out  
498 according to their 91-d protocol.

499

500 **Western blotting**

501 To determine the levels of bacterial and host proteins in purified bacterial samples, 30%-  
502 purified bacterial samples were boiled in 1x SDS loading buffer (150 mM Tris pH 6.8, 6% SDS,

503 0.3% bromophenol blue, 30% glycerol, 15%  $\beta$ -mercaptoethanol) for 10 min, then  $5 \times 10^6$  PFUs  
504 were resolved on an 8-12% SDS-PAGE gel and transferred to an Immobilon-FL polyvinylidene  
505 difluoride membrane (Millipore, IPEL00010). Membranes were probed for 30 min at room  
506 temperature or 4°C overnight with antibodies as follows: affinity-purified rabbit anti-OmpB  
507 antibody (II) diluted 1:200-30000 in TBS-T (20 mM Tris, 150 mM NaCl, pH 8.0, 0.05% Tween  
508 20 (Sigma, P9416)) plus 5% dry milk (Apex, 20-241); mouse monoclonal anti-OmpA 13-3  
509 antibody diluted 1:10000-50000 in TBS-T plus 5% dry milk; rabbit anti-OmpW serum diluted  
510 1:8000 in TBS-T plus 5% dry milk; mouse monoclonal FK1 anti-polyubiquitin antibody diluted  
511 1:2500 in TBS-T plus 2% BSA; rabbit anti-EF-Tu serum diluted 1:15000 in TBS-T plus 5% dry  
512 milk; or rabbit anti-O-antigen serum 1:5000 in TBS-T plus 5% dry milk. Secondary antibodies  
513 were: mouse anti-rabbit horseradish peroxidase (HRP) (Santa Cruz Biotechnology, sc-2357), or  
514 goat anti-mouse HRP (Santa Cruz Biotechnology, sc-2005), all diluted 1:1000-2500 in TBS-T plus  
515 5% dry milk. Secondary antibodies were detected with ECL Western Blotting Detection Reagents  
516 (GE, Healthcare, RPN2106) for 1 min at room temperature, and developed using Biomax Light  
517 Film (Carestream, 178-8207).

518

519 **Immunofluorescence microscopy**

520 *R. parkeri* infections were carried out in 24-well plates with sterile circle 12-mm coverslips  
521 (Thermo Fisher Scientific, 12-545-80). To initiate infection, 30%-purified bacteria were diluted in  
522 cell culture media at room temperature to a MOI of 0.01 for Vero cells, and a MOI of 0.1 for  
523 BMDMs. Bacteria were centrifuged onto cells at 300g for 5 min at room temperature and  
524 subsequently incubated at 33 °C. Next, infected cells were fixed for 10 min at room temperature  
525 in pre-warmed (37 °C) 4% PFA diluted in PBS, pH 7.4, then washed 3 times with PBS. Primary

526 antibodies were the following: for staining with the guinea pig polyclonal anti-p62 antibody  
527 (Fitzgerald, 20R-PP001; 1:500 dilution), mouse polyclonal anti-NDP52 antibody (Novus  
528 Biologicals, H00010241-B01P; 1:100 dilution), a rabbit anti-*Rickettsia* I7205 antibody (1:500  
529 dilution; gift from Ted Hackstadt), or anti-polyubiquitin FK1 antibody (1:250 dilution), cells were  
530 permeabilized with 0.5% Triton-X100 for 5 min prior to staining. For staining with mouse  
531 monoclonal anti-OmpA 13-3 antibody (1:5000 dilution), anti-OmpB antibody (11) (1:1000  
532 dilution), or rabbit anti-O-antigen serum (15) (1:500 dilution), infected cells were post-fixed in  
533 methanol for 5 min at RT (no Triton-X). Cells were then washed 3 times with PBS and incubated  
534 with the primary antibodies for 30 min at RT. To detect the primary antibodies, secondary goat  
535 anti-rabbit Alexa-568 (Invitrogen, A11036), goat anti-mouse Alexa-568 (Invitrogen, A11004), or  
536 goat anti-guinea pig Alexa-568 (Invitrogen, A11075), Alexa 488 anti-rabbit antibody (Invitrogen,  
537 A11008; 1:500 dilution), Alexa 488 anti-mouse antibody (Invitrogen, A11001) antibodies were  
538 incubated at room temperature for 30 min (all 1:500 in PBS with 2% BSA). Images were captured  
539 as 15-25 z-stacks (0.1- $\mu$ m step size) on a Nikon Ti Eclipse microscope with a Yokogawa CSU-XI  
540 spinning disc confocal with 100x (1.4 NA) Plan Apo objectives, and a Clara Interline CCD Camera  
541 (Andor Technology) using MetaMorph software (Molecular Devices). Images were processed  
542 using ImageJ using z-stack average maximum intensity projections and assembled in Adobe  
543 Photoshop. For quantification of the percentage of bacteria with pUb and p62, only bacteria that  
544 co-localized with rim-like patterns of the respective marker were scored as positive for staining.  
545 To quantify pUb, p62, NDP52, OmpB, and OmpA signal per bacteria, z-stacks were projected as  
546 stated above, and the edges of individual bacteria were marked by the freehand region of interest  
547 (ROI) function in ImageJ. Subsequently, the average pixel intensity within that ROI was measured.  
548 pUb/p62/NDP52 signal intensities were calculated by subtracting the average pUb/p62/NDP52

549 signal of WT bacteria from the pUb/p62/NDP52-value of each bacterium. OmpB signal intensity  
550 was calculated by subtracting the average OmpB-signal of *ompB<sup>STOP</sup>::tn* bacteria from the OmpB-  
551 value of each bacterium. OmpA signal intensity was calculated by subtracting the average  
552 background-signal (areas with no bacteria) from the OmpA-value of each bacterium.

553

#### 554 **Sample preparation for mass spectrometry to determine the lysine methylome**

555  $5 \times 10^7$  gradient-purified WT (Passage 6), *pkmt1::tn* (P4) and *pkmt2::tn* (P4) bacteria were  
556 centrifuged at 11,000g for 3 min. Each pellet was resuspended in 50  $\mu$ L Tris (10 mM)-EDTA (10  
557 mM), pH 7.6, and incubated for 45 min in a 45 °C water bath. Bacterial surface fractions were  
558 recovered from the supernatant after centrifugation at 11,000g for 3 min. Pellet was resuspended  
559 as above and incubated for additional 45 min at 45 °C before resuspension in 50  $\mu$ L Tris (10 mM)-  
560 EDTA (10 mM). Both pellet and surface fractions were boiled at 95 °C for 10 min. Samples were  
561 cooled to RT prior to addition of 20  $\mu$ L 50 mM NH<sub>4</sub>HCO<sub>3</sub>, pH 7.5, and 50  $\mu$ L of a 0.2% solution  
562 of RapiGest (diluted in NH<sub>4</sub>HCO<sub>3</sub>, Waters, 186001861). Next, samples were heated at 80 °C for  
563 15 min and cooled to RT before addition of 1  $\mu$ g of trypsin (Promega, V511A). Samples were  
564 digested at 37 °C overnight. To hydrolyze the RapiGest, 20  $\mu$ L of 5% trifluoroacetic acid (TFA)  
565 was added to samples which were incubated at 37 °C for 90 min prior centrifugation at 15000g for  
566 25 min at 4 °C. Samples were desalted using C18 OMIX tips (Agilent Technologies, A57003100)  
567 according to the manufacturer's instructions and sample volume was decreased to 20  $\mu$ L using a  
568 SpeedVac vacuum concentrator. Samples were stored at 4 °C prior to analysis.

569

#### 570 **TUBE assay and sample preparation for mass spectrometry**

571 To enrich for polyubiquitylated proteins, 3x10<sup>8</sup> PFUs of “purified” WT (P6), *ompB<sup>STOP</sup>::tn*  
572 (P6) and *pkmt1::tn* (P4) and *pkmt2::tn* (P3) bacteria were centrifuged at 14,000g for 3 min at room  
573 temperature. Next, to release the surface protein fraction, the bacterial pellets were resuspended in  
574 lysis buffer (50 mM Tris-HCl, pH 7.5, 150 mM NaCl, 1 mM EDTA and 10% glycerol),  
575 supplemented with 0.0031% v/v lysonase (Millipore, 71230), the deubiquitylase inhibitor PR619  
576 (Life Sensor, SI9619) at a final concentration of 20 µM, and 0.8% w/v octyl β-D-glucopyranoside  
577 (Sigma, O8001), and incubated on ice for 10 min with occasional pipetting of samples to break  
578 pellet into smaller pieces. Subsequently, the lysate was cleared by centrifugation at 14,000g at 4  
579 °C for 5 min and incubated with equilibrated agarose TUBE-1 (Life Sensor, UM401) for 3 h, at 4  
580 °C. After binding of polyubiquitylated proteins to TUBE-1, agarose beads were washed 1 time  
581 with TBS supplemented with 0.05% Tween and 5 mM EDTA, and subsequently 3 times with TBS  
582 only (no Tween or EDTA) and centrifuged at 5,000g for 5 min. To prepare samples for MS  
583 analysis, enriched proteins were digested at 37 °C overnight on agarose beads in RapiGest SF  
584 solution (Waters, 186001861) supplemented with 0.75 µg trypsin (Promega, V511A). The reaction  
585 was stopped using 1% TFA (Sigma, T6508). Octyl β-D-glucopyranoside was extracted using  
586 water-saturated ethyl acetate (Sigma, 34858). Prior to submission of samples for mass  
587 spectrometry analysis, samples were desalted using C18 OMIX tips (Agilent Technologies,  
588 A57003100), according to the manufacturer’s instructions.

589

## 590 **Liquid chromatography-mass spectrometry**

591 Samples of proteolytically digested proteins were analyzed using a Synapt G2-Si ion  
592 mobility mass spectrometer that was equipped with a nanoelectrospray ionization source (Waters).  
593 The mass spectrometer was connected in line with an Acquity M-class ultra-performance liquid

594 chromatography system that was equipped with trapping (Symmetry C18, inner diameter: 180  $\mu\text{m}$ ,  
595 length: 20 mm, particle size: 5  $\mu\text{m}$ ) and analytical (HSS T3, inner diameter: 75  $\mu\text{m}$ , length: 250  
596 mm, particle size: 1.8  $\mu\text{m}$ ) columns (Waters). Data-independent, ion mobility-enabled, high-  
597 definition mass spectra and tandem mass spectra were acquired in the positive ion mode (23-25).  
598 Raw data acquisition was controlled using MassLynx software (version 4.1), and tryptic peptide  
599 identification and relative quantification using a label-free approach (26, 27) were performed using  
600 Progenesis QI for Proteomics software (version 4.0, Waters). Raw data were searched against  
601 *Rickettsia parkeri* and *Chlorocebus sabaeus* protein databases (National Center for Biotechnology  
602 Information, NCBI) to identify tryptic peptides, allowing for up to three missed proteolytic  
603 cleavages, with diglycine-modified lysine (i.e., ubiquitylation remnant) and methylated lysine as  
604 variable post-translational modifications. Calculation of the percentage of lysine methylation  
605 (mono, di, tri or unmethylated), for each bacterial strain, was performed by dividing the abundance  
606 of a residue/protein bearing a modification by the total abundance and multiplying by 100. Data-  
607 dependent analysis was performed using an UltiMate3000 RSLCnano liquid chromatography  
608 system that was connected in line with an LTQ-Orbitrap-XL mass spectrometer equipped with a  
609 nanoelectrospray ionization source, and Xcalibur (version 2.0.7) and Proteome Discoverer  
610 (version 1.3, Thermo Fisher Scientific, Waltham, MA) software, as described elsewhere (28).  
611

## 612 **Localization of tagged ubiquitin and ubiquitin pull-downs**

613 To assess localization of 6xHis-ubiquitin during infection, confluent Vero cells grown in  
614 24-well plates with coverslips were transfected with 2  $\mu\text{g}$  of pCS2-6xHis-ubiquitin plasmid DNA  
615 using Lipofectamine 2000 (Invitrogen, 11668-019) for 6 h in Opti-MEM (Gibco, 31985-070).  
616 Subsequently, media were exchanged to media without transfection reagent, and cells were

617 incubated overnight at 37 °C and 5% CO<sub>2</sub>. The following day (~16 h after transfection), transfected  
618 cells were infected with purified WT or mutant bacteria at a MOI of 1. At 28 h.p.i., infected cells  
619 were fixed with 4% PFA diluted in PBS, pH 7.4 for 10 min, then washed 3 times with PBS. Primary  
620 anti-6xHis monoclonal mouse antibody (Clontech, 631212, diluted 1:1,000) was used to detect  
621 6xHis-ubiquitin in samples permeabilized with 0.5% Triton-X100, and a goat anti-mouse Alexa-  
622 568 (Invitrogen, A11004) to detect the primary 6xHis antibody. Hoechst (Thermo Scientific,  
623 62249, diluted 1:2500) was used to detect host and bacterial DNA. Samples were imaged as  
624 already described.

625 For ubiquitin pull-downs, confluent Vero cells grown in 6-well plates were transfected and  
626 infected as described above. At 28 h.p.i., cells were washed once with 1x PBS, pH 7.4, and  
627 subsequently lysed in urea lysis buffer (8 M urea, 50 mM Tris-HCl, pH 8.0, 300 mM NaCl, 50  
628 mM Na<sub>2</sub>HPO<sub>4</sub>, 0.5% Igepal CA-630 (Sigma, I8896)) for 20 min at RT. Subsequently, samples  
629 were sonicated, and lysate was cleared by centrifugation at 15000g for 15 min at room temperature.  
630 Prior to incubation with Ni-NTA resin, an aliquot was saved for the input sample. 6xHis-ubiquitin  
631 conjugates were purified by incubation and rotation with Ni-NTA resin for 3 h, at RT, in the  
632 presence of 10 mM imidazole. Beads were washed 3 times with urea lysis buffer and 1 time with  
633 urea lysis buffer lacking Igepal CA-630. Ubiquitin conjugates were eluted at 65 °C for 15 min in  
634 2x Laemmli buffer containing 200 mM imidazole and 5% 2-mercaptoethanol (Sigma, M6250),  
635 vortexed for 90 seconds, and centrifuged at 5000g for 5 min at RT. Eluted and input proteins were  
636 detected by SDS-PAGE followed by western blotting, as described above.

637

638 **Animal experiments**

639                   Animal research using mice was conducted under a protocol approved by the UC Berkeley  
640                   Institutional Animal Care and Use Committee (IACUC) in compliance with the Animal Welfare  
641                   Act. The UC Berkeley IACUC is fully accredited by the Association for the Assessment and  
642                   Accreditation of Laboratory Animal Care International and adheres to the principles of the Guide  
643                   for the Care and Use of Laboratory Animals. Infections were performed in a biosafety level 2  
644                   facility. Mice were age-matched between 8 and 18 weeks old. Mice were selected for experiments  
645                   based on their availability, regardless of sex. All mice were healthy at the time of infection and  
646                   were housed in microisolator cages and provided chow and water. Littermates of the same sex  
647                   were randomly assigned to experimental groups. For infections, *R. parkeri* was prepared by  
648                   diluting 30%-prep bacteria into cold sterile 1x PBS to  $5 \times 10^6$  PFU per 200 mL. Bacterial  
649                   suspensions were kept on ice during injections. Mice were exposed to a heat lamp while in their  
650                   cages for approximately 5 min, and then each mouse was moved to a mouse restrainer (Braintree,  
651                   TB-150 STD). The tail was sterilized with 70% ethanol, and 200  $\mu$ L of bacterial suspensions were  
652                   injected using 30.5-gauge needles into the lateral tail vein. Body temperatures were monitored  
653                   using a rodent rectal thermometer (BrainTree Scientific, RET-3). Mice were monitored daily for  
654                   clinical signs of disease, such as hunched posture, lethargy, or scruffed fur. If a mouse displayed  
655                   severe signs of infection, as defined by a reduction in body temperature below 90 °F or an inability  
656                   to move around the cage normally, the animal was immediately and humanely euthanized using  
657                   CO<sub>2</sub> followed by cervical dislocation, according to IACUC-approved procedures (16).  
658

#### 659                   **Statistical analysis, experimental variability and reproducibility**

660                   Statistical parameters and significance are reported in the legends. Data were considered  
661                   to be statistically significant when  $p < 0.05$ , as determined by a one-way ANOVA with Dunnett's

662 post-hoc test, a Kruskal-Wallis test with Dunn's post-hoc test, a Brown-Forsyth and Welch  
663 ANOVA with Dunnett's post-hoc test, or a two-way ANOVA (all two-sided). Statistical analysis  
664 was performed using PRISM 6 software (GraphPad Software). If not otherwise described,  $n$   
665 indicates the number of independent biological experiments executed at different times.